Particle acceleration, pair creation and gamma-ray emission of pulsars

K.S. Cheng

Department of Physics

University of Hong Kong

Hong Kong, China

Co-workers
Jumpei Takata
Yu Wang

- Introduction
- Particle acceleration region – gaps
- Simple 2D model for gamma-ray emission of Fermi pulsars
- A magnetic pair creation model for gamma-ray pulsars
- Summary

Stellar Evolution

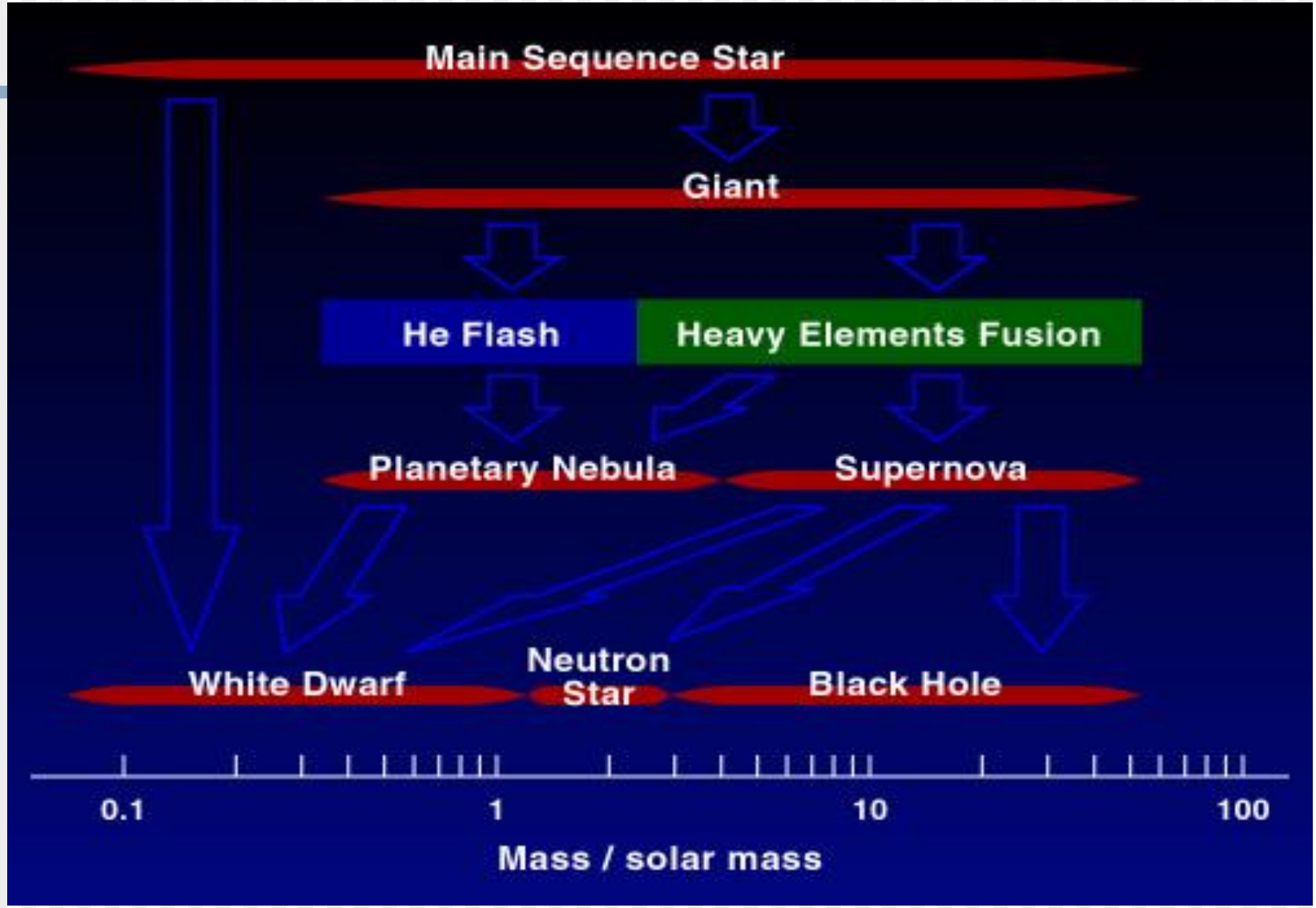

Pulsars

- In the past, physicists did not take the existence of neutron stars seriously because (1)could such stellar object stable ? And (2)such tiny stellar objects will be very difficult to be detected.
- In 1967, Cambridge astronomers Hewish et al. detected some very intense but extremely regular radio signals from the sky
- This is the known pulsar as CP1919 with period 1.337s

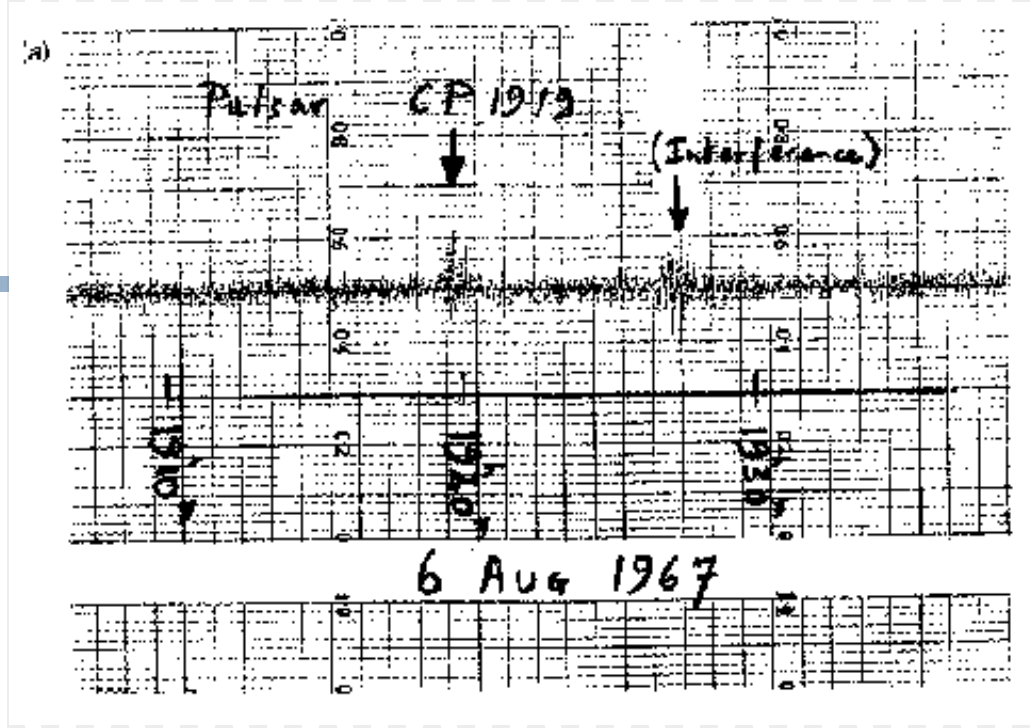

Why are pulsars powerful radiation sources?

- Pulsars are rotating and strongly magnetized objects, so they can act like unipolar inductor
- The maximum potential drop can be as large as $V_{\max} \approx 6.6 \times 10^{12} B_{12} P^{-2} volts$
- For young pulsars, the maximum potential can be much higher than 10^{15} volts
- This potential drop can accelerate charged particles and radiate high energy photons from various accelerators in the magnetosphere

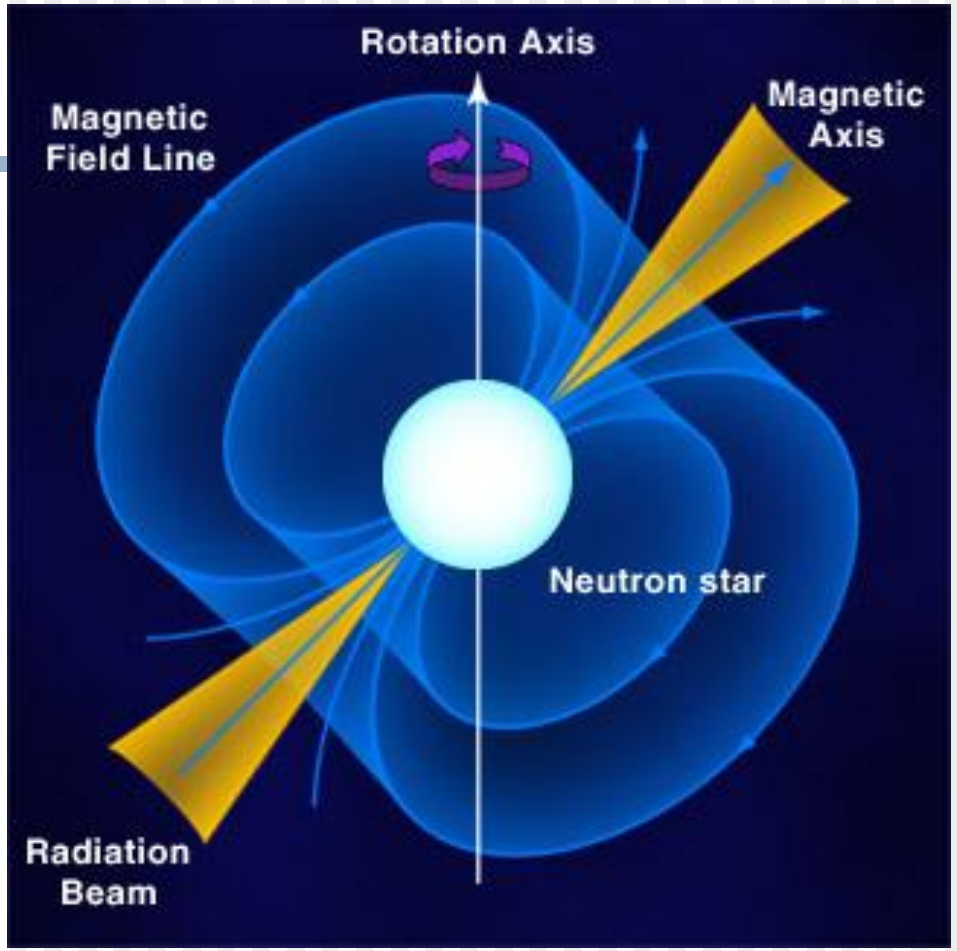

Gamma-ray Emission Models

Different theoretical models try to explain the observed gamma-ray emission.

They assume different origin in the magnetosphere => different emission geometry.

Depending on:

α: angle between magnetic and rotation axis

β: angle between line-of-sight and magnetic axis

Different emission patterns are expected (number of peaks, separation, radio/gamma lag, ratio of radio-loud/radio-quiet).

Gamma-ray observations can help us to differentiate the geometry of pulsars.

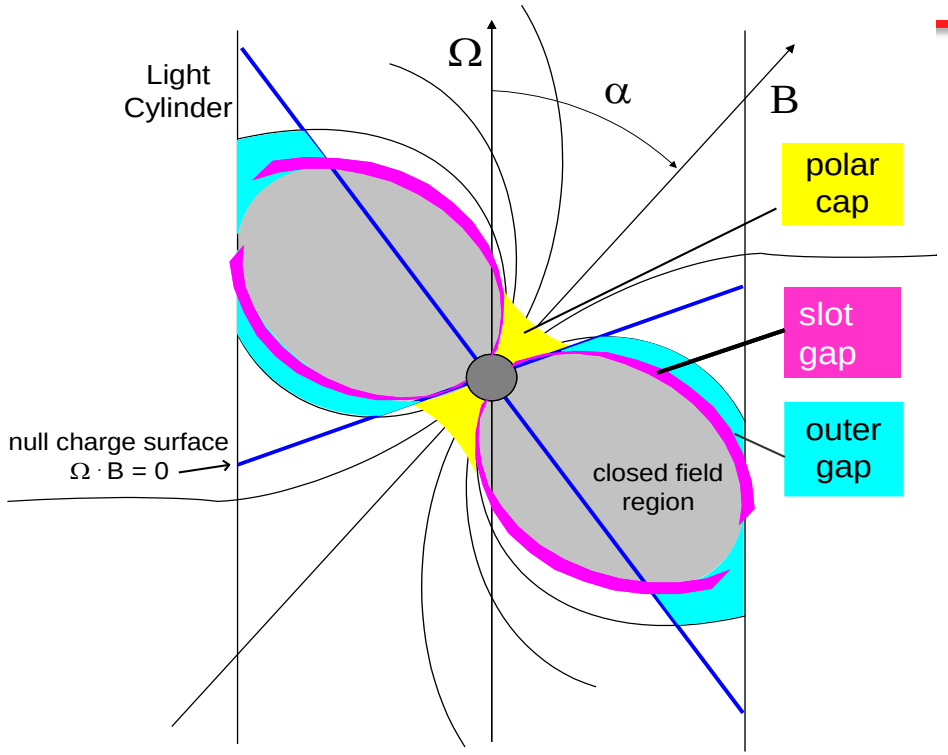

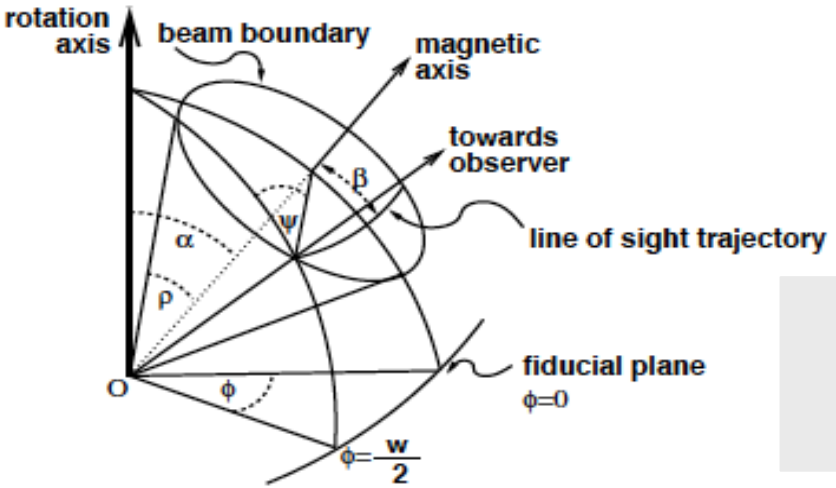

Multi-wavelength emission from EGRET gamma-ray pulsars

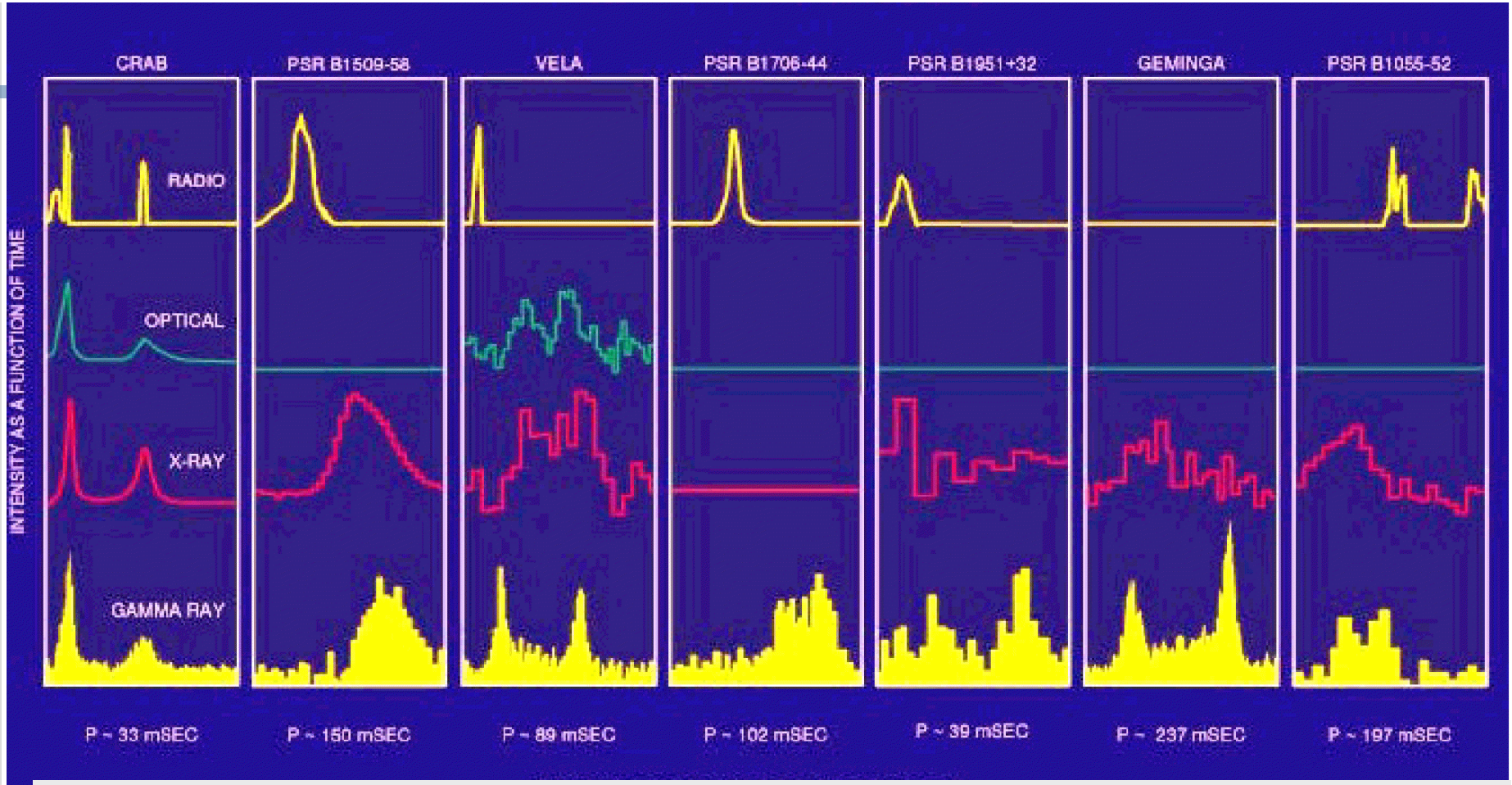

It is predicted that radio-quiet gamma-ray pulsars should be more than radio-loud gamma-ray pulsars due to narrow radio beam plus low efficiency in radio band(e.g. Cheng et al.1998)

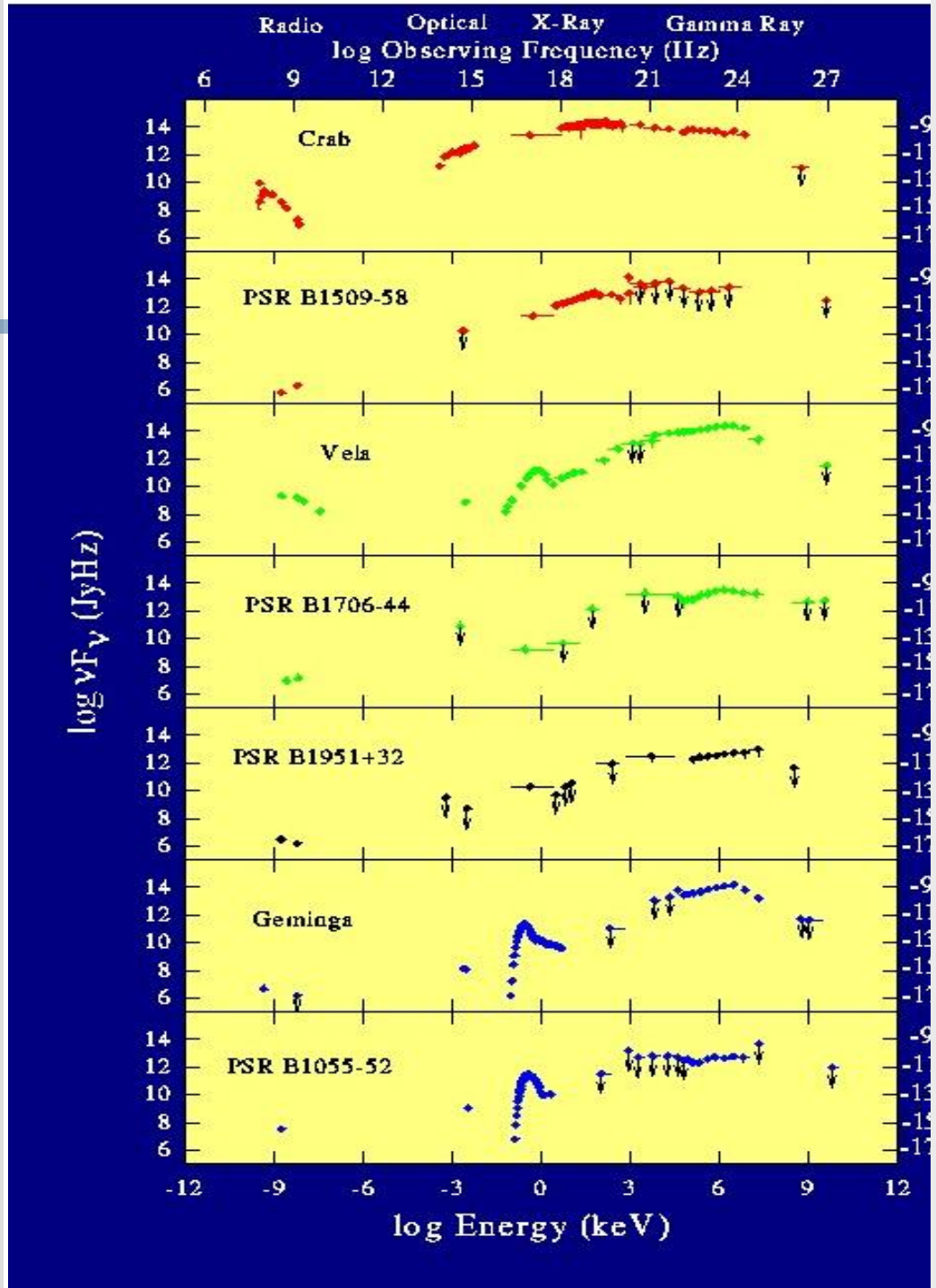

Broad-band spectra

- Power peaked in γ-rays
- No pulsed emission above 20 GeV (This statement is no longer true, at least Crab pulsar and may be Vela have 20GeV photons)
- High-energy turnover
- Increase in hardness with age
- Thermal component appears in older pulsars


Fermi
Gamma-ray Space Telescope
NASA
National Aeronautics and Space Administration
www.nasa.gov/fermi

Fermi Satellite –The Gamma-ray Large Space Telescope (GLAST launch 11/6/2008)

The Large Area Telescope (LAT) on the Fermi Gamma-ray Space Telescope

- Pair production telescope with silicon tracker, CsI calorimeter, and segmented anti-coincidence detector
  - 20 MeV to >300 GeV
  - 8000 cm^2 area (at 1 GeV)
  - 0.6–0.8 deg radius PSF (1 GeV)
- Continuous sky survey mode of operation
- Big improvement in area, FOV, and reduction in background compared to EGRET

(Ray 2010)

One year sky map of Fermi > 1000 sources!

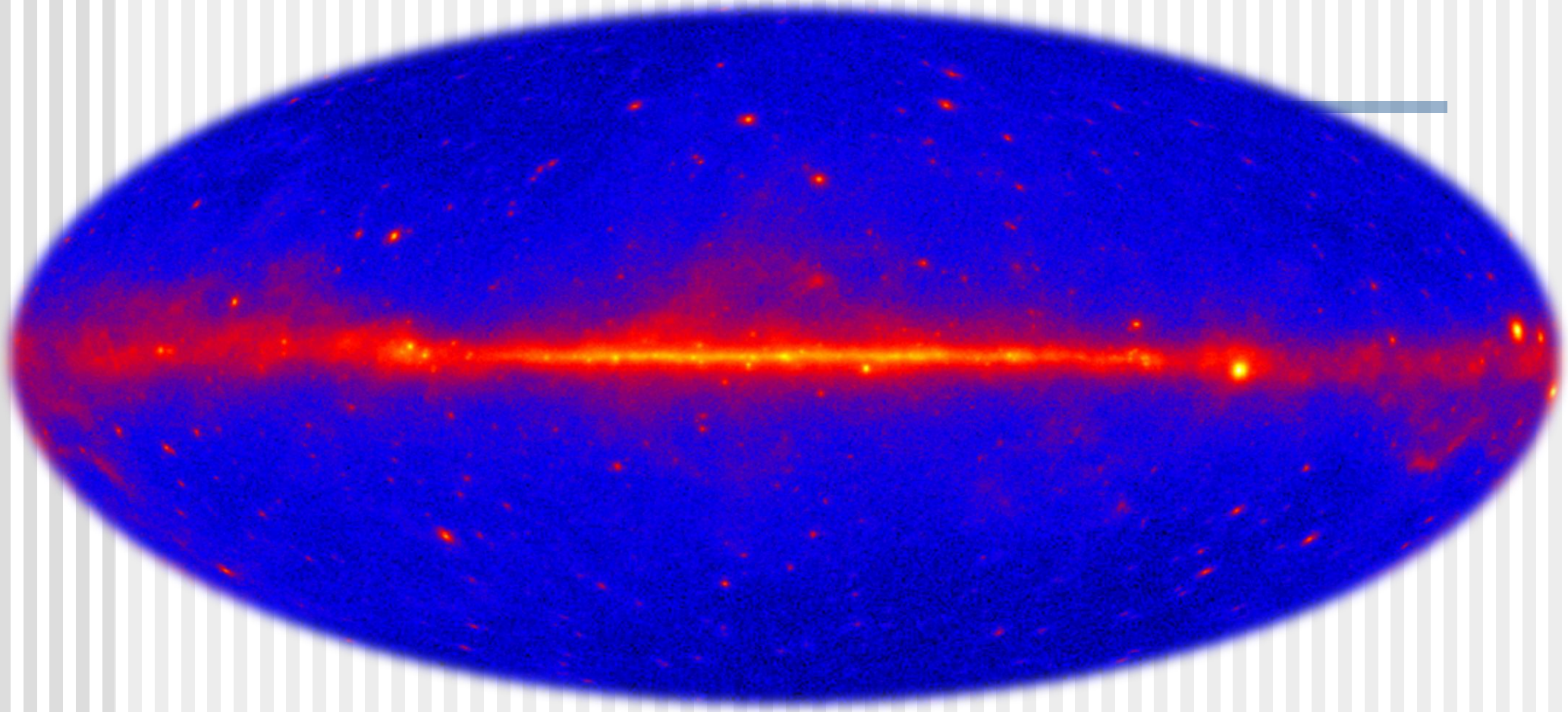

Abdo et al, 2009, ApJS, 183, 46

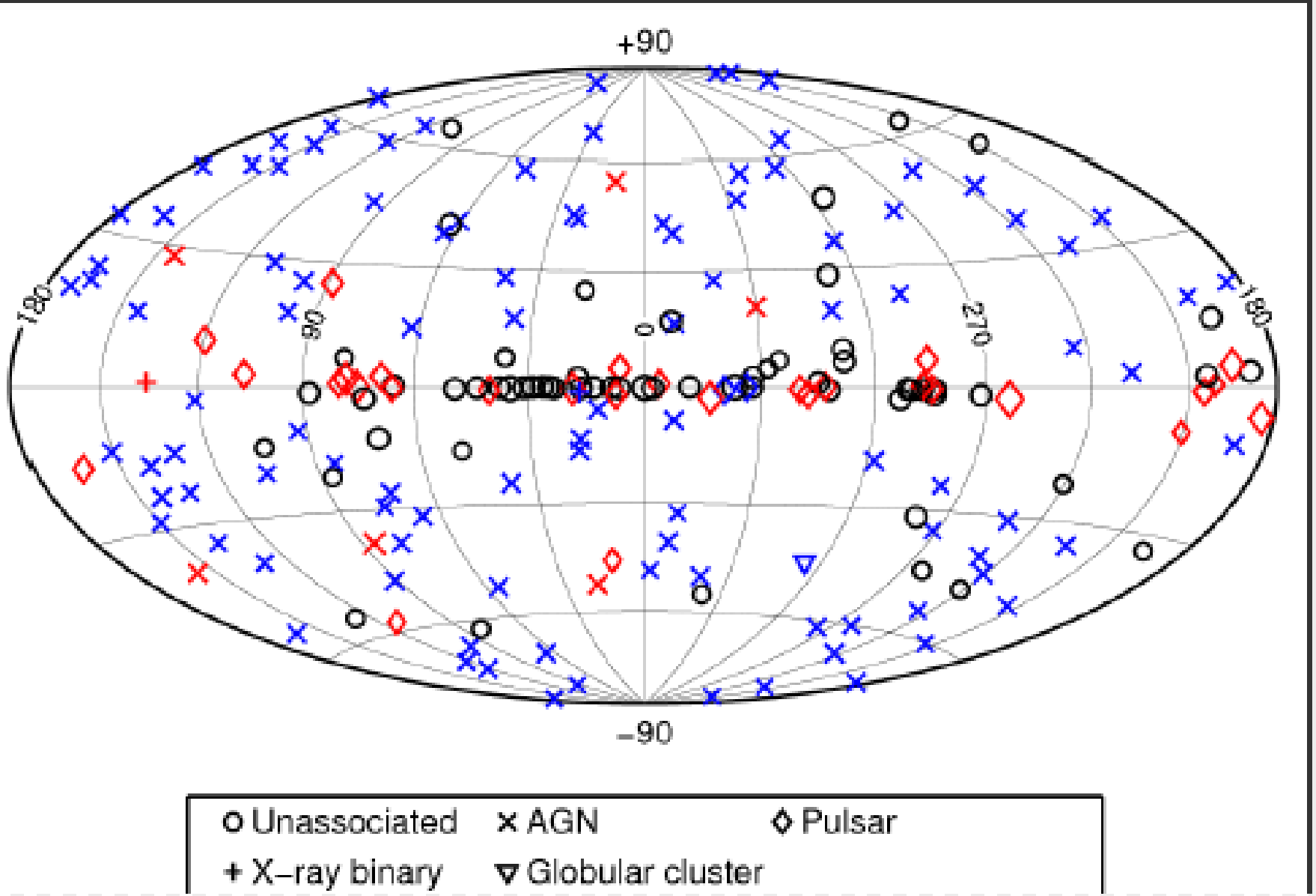

The pulsar catalog

In addition to the search for new pulsars, 762 known pulsars with ephemerides were searched for pulsations in nine months of data.

=> 46 pulsars were detected: 16 blind search PSRs, 8 radio-loud MSPs, 22 radio-loud normal PSRs.

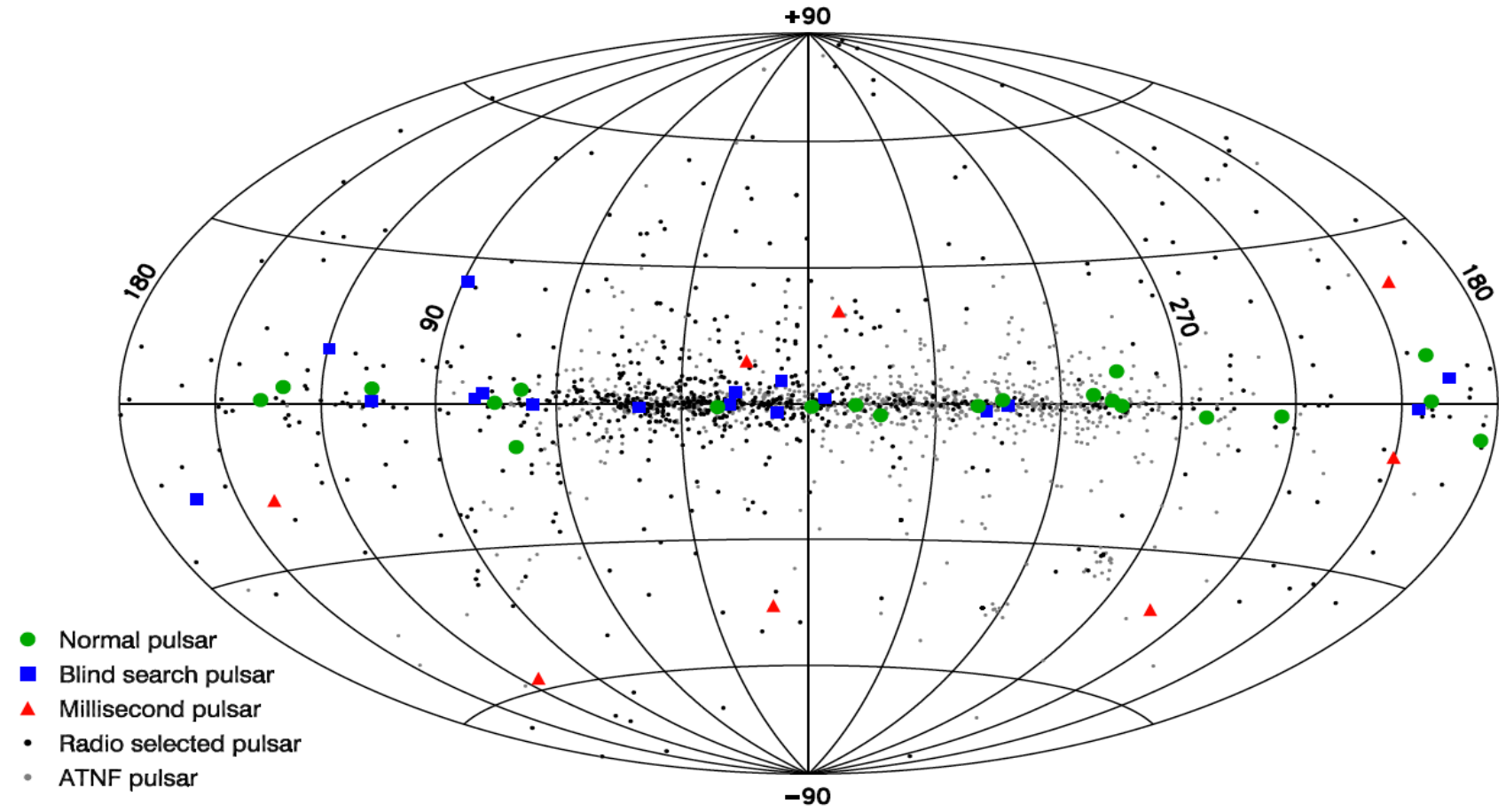

L. Guillemot, 2009 Fermi Symposium, 2 November 2009

Early Fermi MSPs and Blind Search PSRs

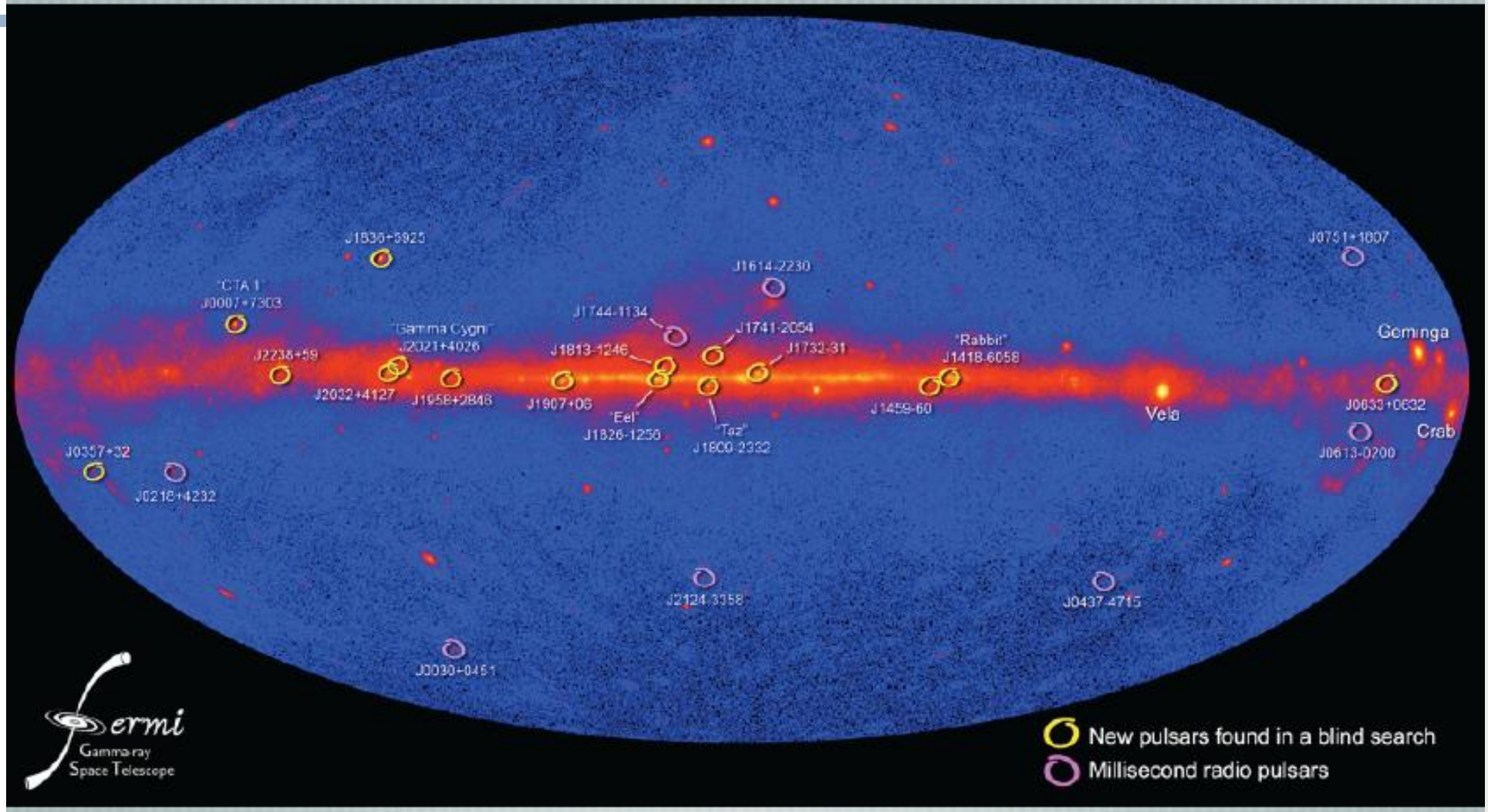

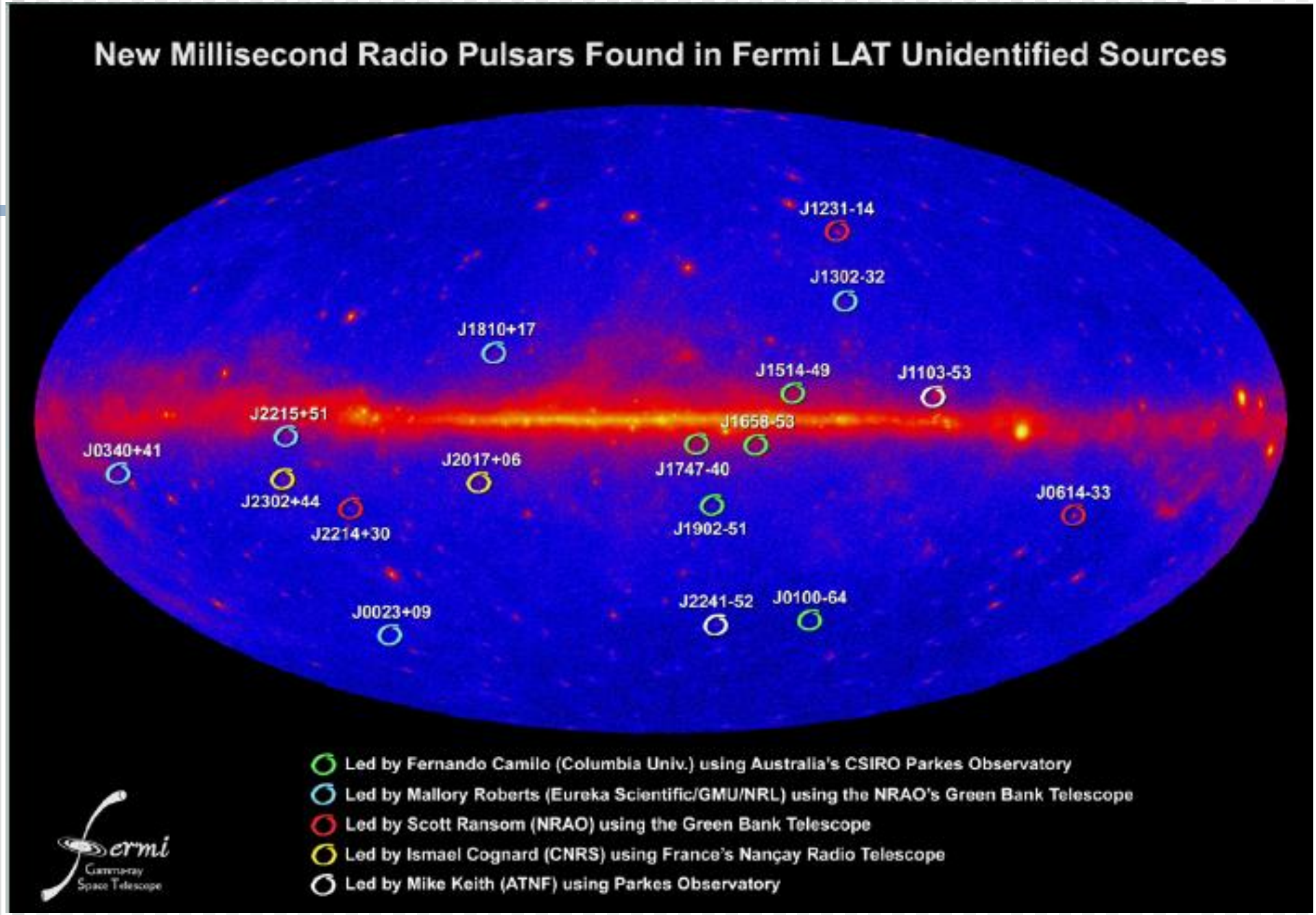
New Millisecond Radio Pulsars Found in Fermi LAT Unidentified Sources
J1231-14
J1302-32
J1810+17
J1514-49
J1103-53
J2215+51
J1658-53
J0340+41
J2017+06
J1747-40
J2302+44
J0614-33
J2214+30
J1902-51
J2241-52
J0100-64
J0023+09
Led by Fernando Camilo (Columbia Univ.) using Australia's CSIRO Parkes Observatory
Led by Mallory Roberts (Eureka Scientific/GMU/NRL) using the NRAO's Green Bank Telescope
Led by Scott Ransom (NRAO) using the Green Bank Telescope
Led by Ismael Cognard (CNRS) using France's Nançay Radio Telescope
Led by Mike Keith (ATNF) using Parkes Observatory
Fermi
Gamma-ray
Space Telescope

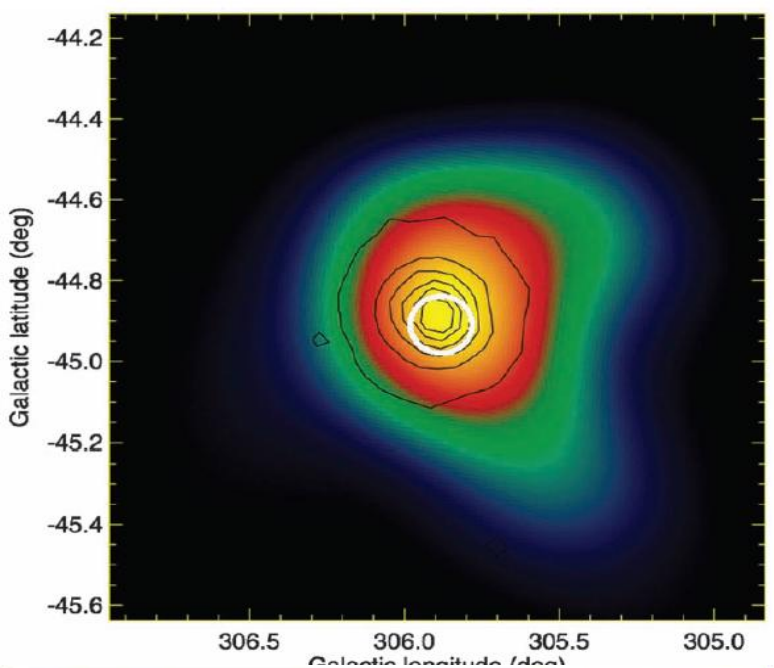

The upper image is the 47 Tucanae. If the gamma-rays of the cluster result from the magnetospheric emission of indidvial pulsars, the implied number of MSPs is ~60.

(Abdo et al., Science 325, 845, 2009)

The bottom image is the Terzan 5, it indicates that the spectrum can extend beyong 10GeV

So far totally 8 globular clusters are detected by Fermi.

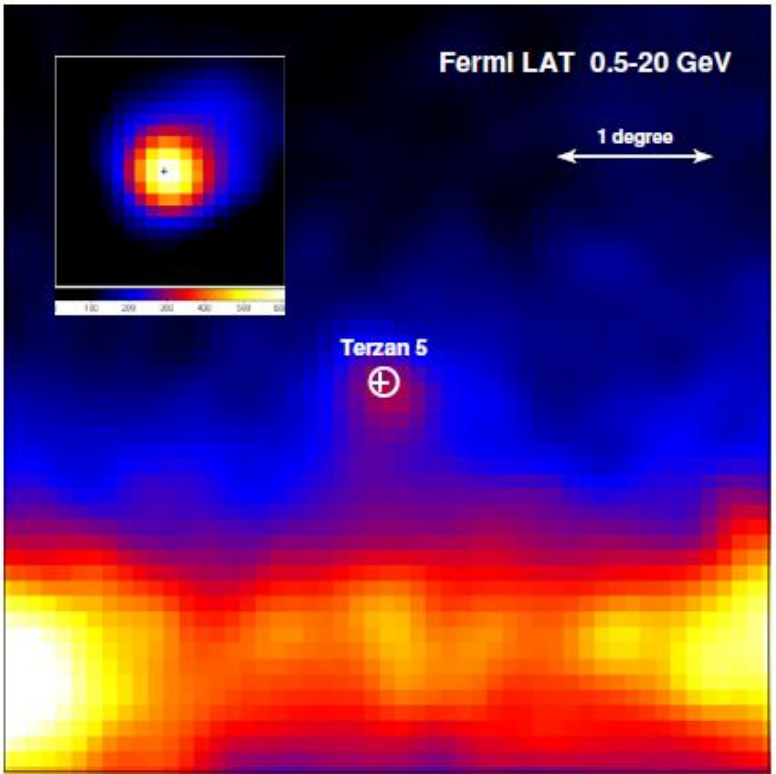

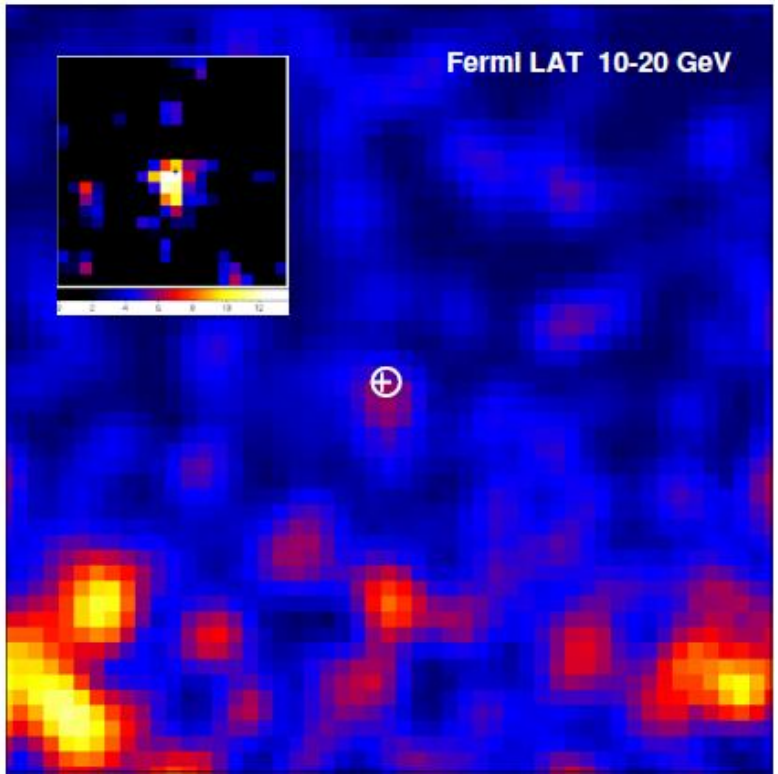

Kong et al. 2010, ApJL

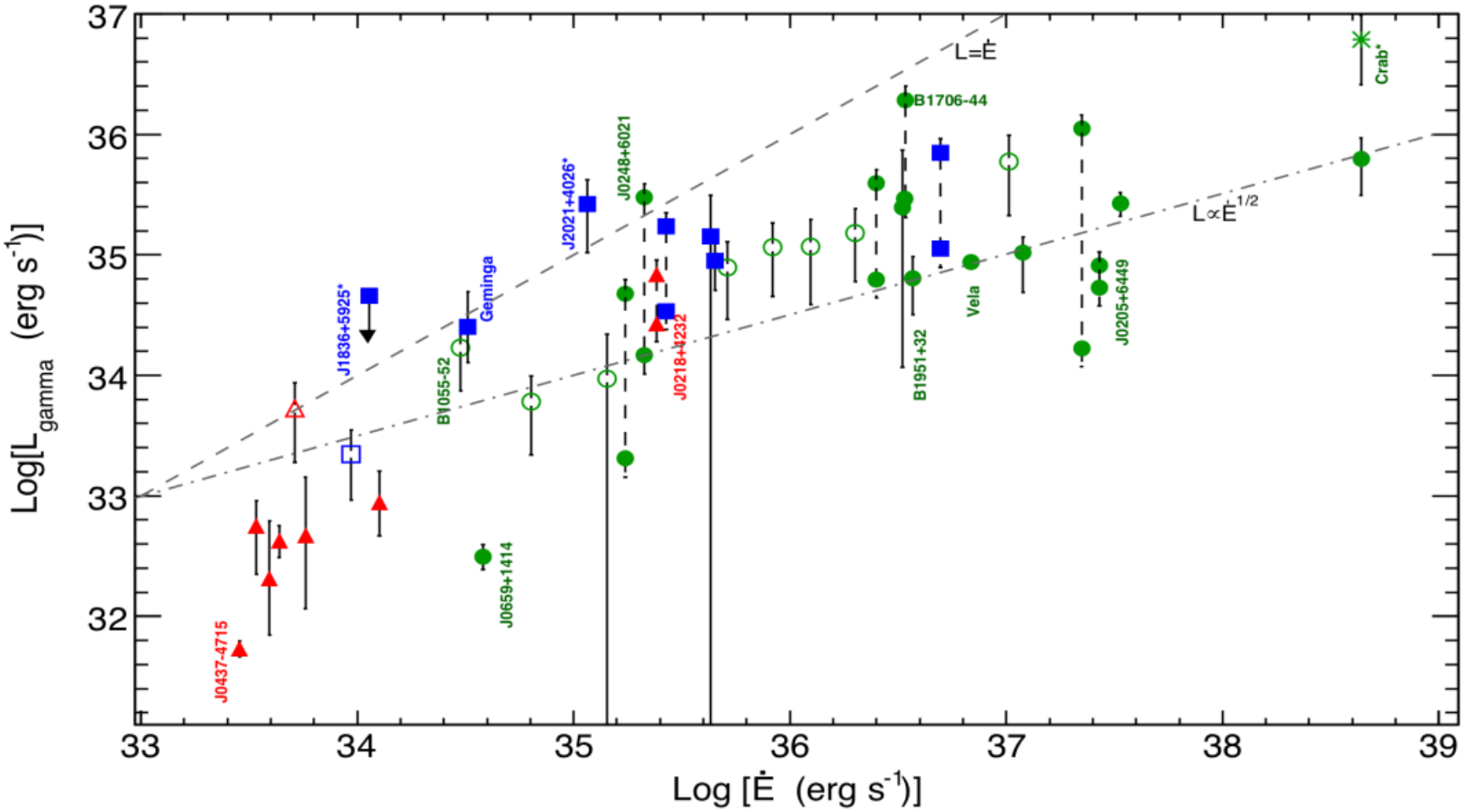

(Abdo et. Al. 2009) The gamma-ray luminosity seems to grow with spin-down power of pulsars; with a $L \propto \dot{E}$ at low $\dot{E}$, $L \propto \sqrt{\dot{E}}$ at high $\dot{E}$. N.B.the gamma-ray power depends sensitively on the real distance to the pulsar.

Pulsar magnetosphere

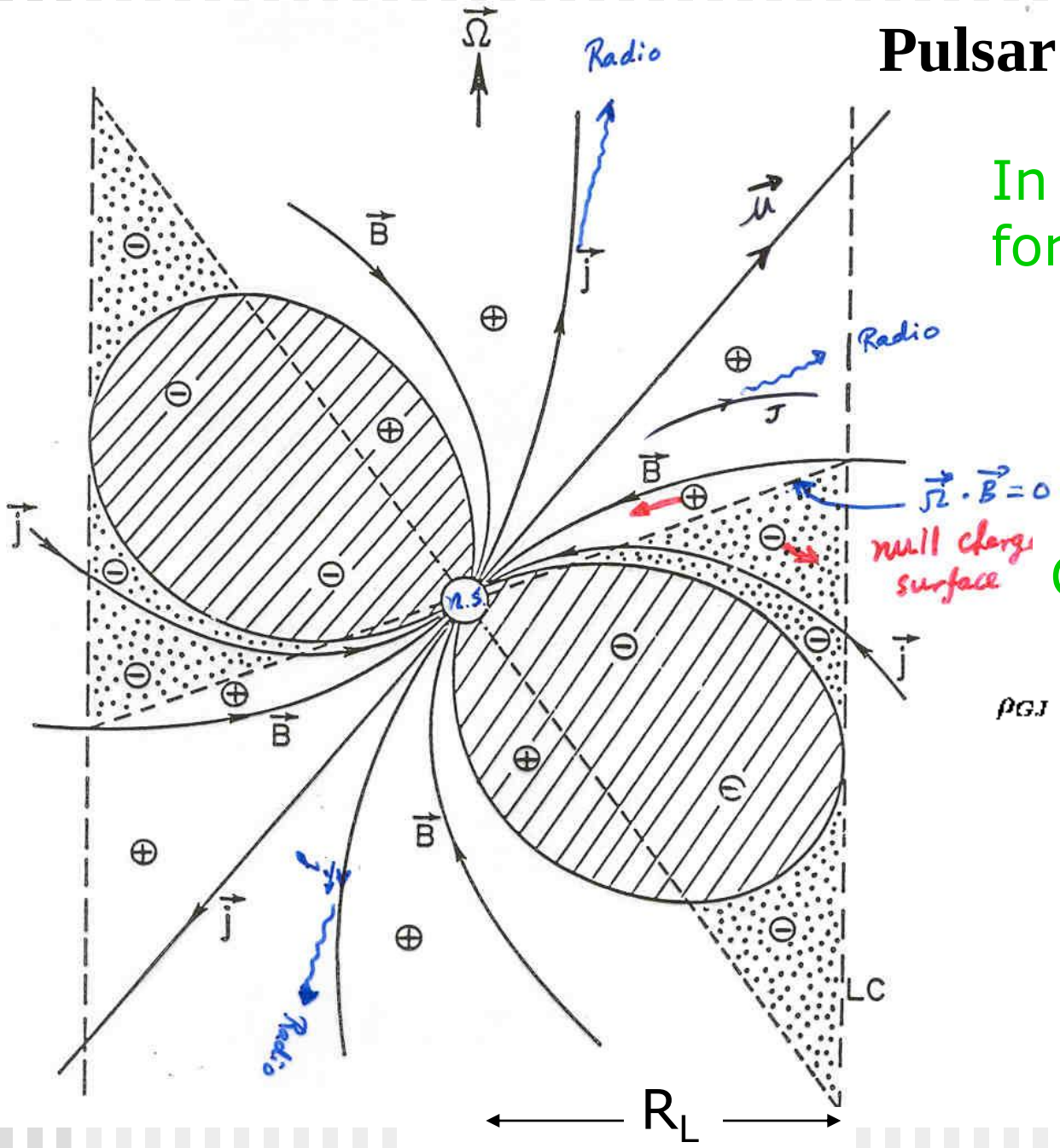

In equilibrium the Lorentz force is assumed to be

$$\mathbf{E} + \frac{1}{c}(\mathbf{\Omega} \times \mathbf{r}) \times \mathbf{B} = 0$$

Charge distribution:

$$\rho_{GJ} = \frac{1}{4\pi}\nabla \cdot \mathbf{E} \approx -\frac{\mathbf{\Omega}\cdot\mathbf{B}}{2\pi c}\frac{1}{1-|\mathbf{\Omega}\times\mathbf{r}/c|^2} \approx -\frac{\mathbf{\Omega}\cdot\mathbf{B}}{2\pi c}$$

Goldreich-Julian charge density

Pair creation in Outergap

When the gap becomes large enough, the energy of curvature photons emitted by the charged particles in the gap can become pairs by

$$\gamma + \gamma(\text{e.g. soft x-rays from stellar surface}) \rightarrow e^{\pm}$$

These pairs limit the growth of the gap

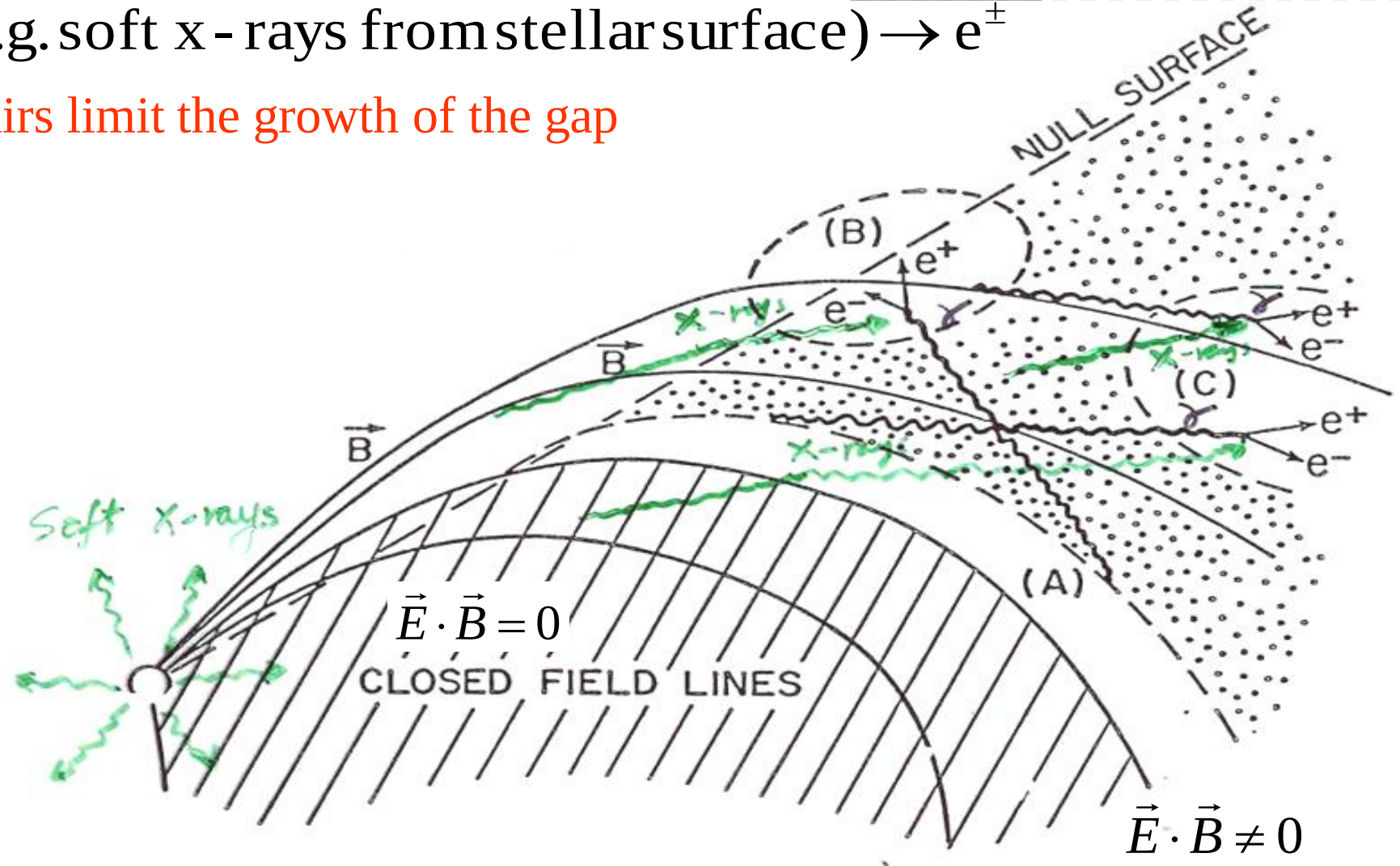

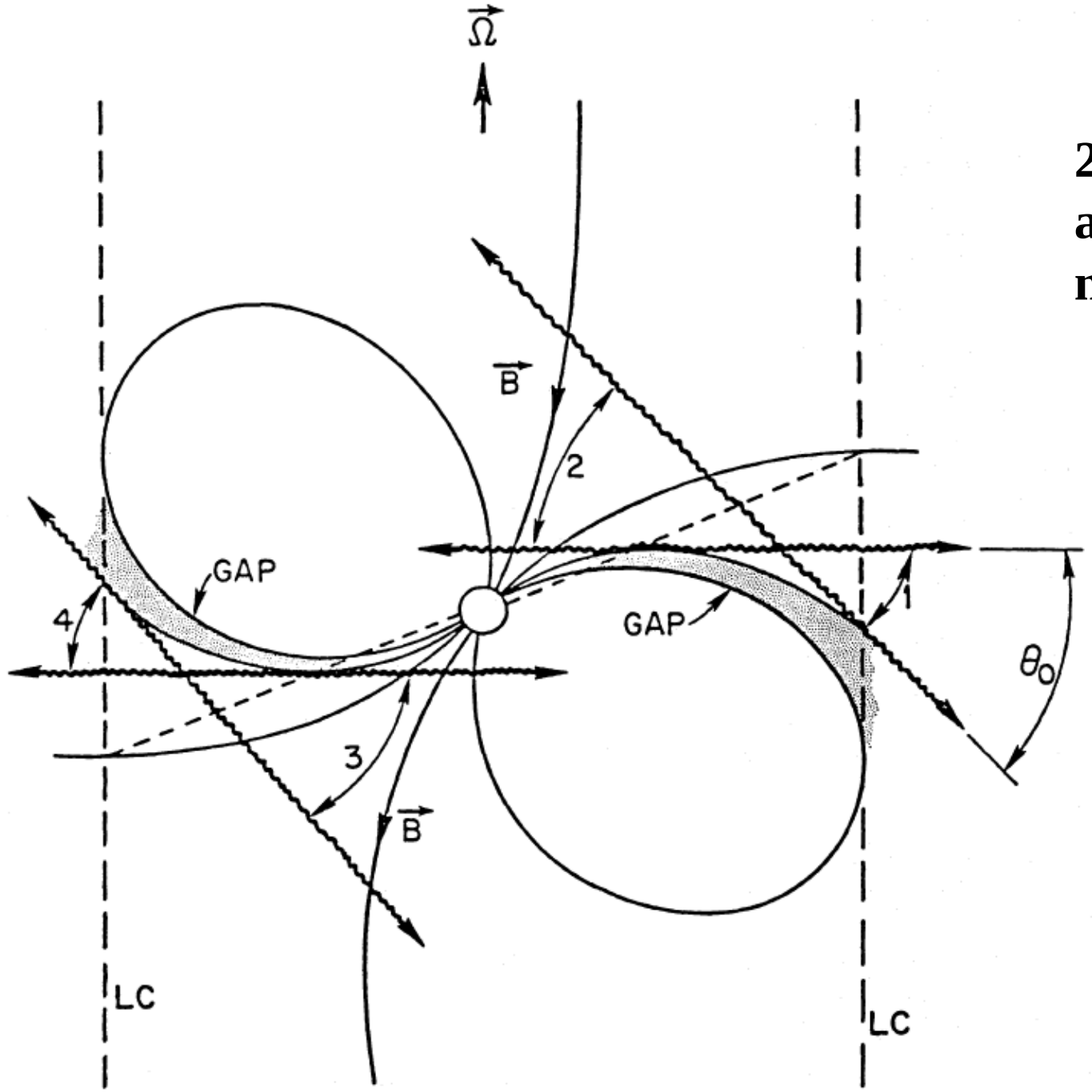

2D structure of the accelerators in the magnetosphere

Cheng, Ho and Ruderman 1986

Static gap

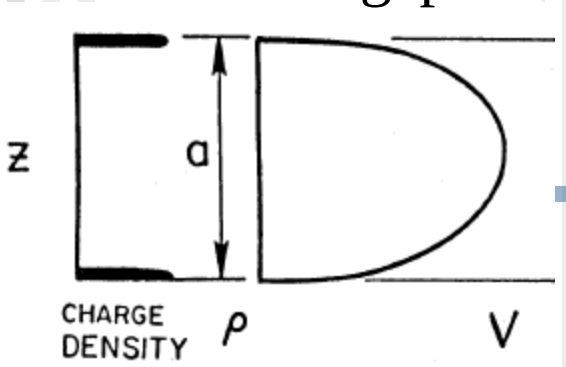

Dynamic gap with pair creation

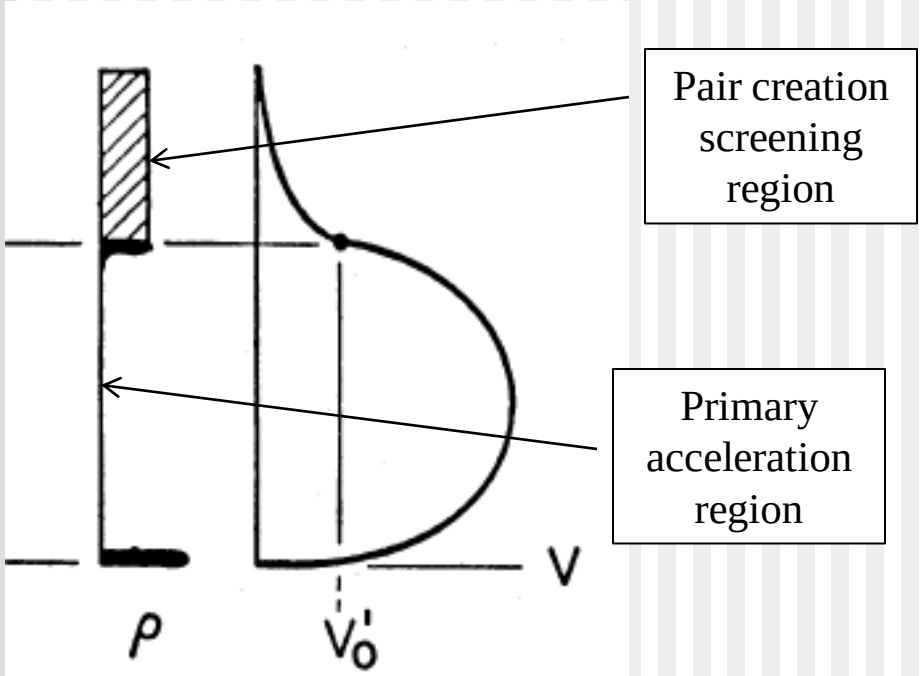

Wang, Takata and Cheng 2010

Approximate charge distribution

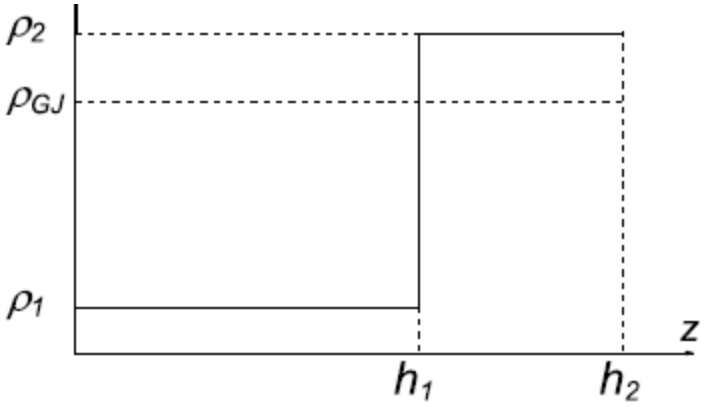

Gap potential

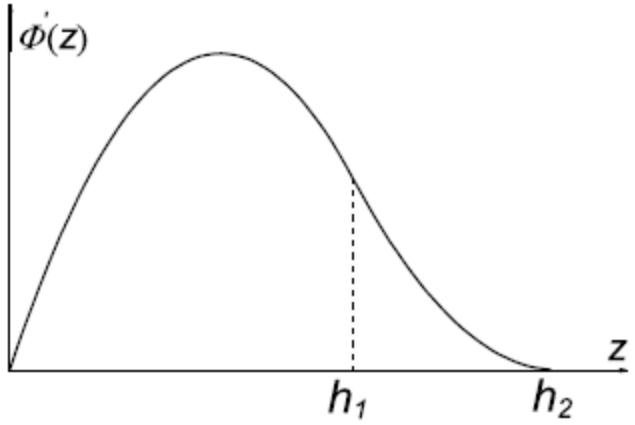

(d)

Solution of the 2D gap potential

$$\left(\frac{\partial^2}{\partial x^2}+\frac{\partial^2}{\partial z^2}\right)\Phi' = -4\pi(\rho-\rho_{GJ})$$ Poisson equation

We approximate the deviation of charge density as $\rho - \rho_{GJ} \sim g(z)\rho_{GJ}(x)$

By introducing $\Phi'(x,z) = \rho_{GJ}(x)\Phi'_z(z)$

We reduce to a 1-D Poisson eq. $\frac{\partial^2}{\partial z^2}\Phi'_z(z) = -4\pi g(z)$

The electric field along field $E_{||} = -\partial\Phi'(x,z)/\partial x$

It is constant for same "z"

Boundary conditions : potential vanishes at z=0 and z=h_2, continues at h_1 and E_x =0 at (0,h_2)

Total parameters : the size of primary "P", screening region "S" size, gap current in "P", gap current in "S" but only three of them or their combinations of them are independent due to the gap closure condition $E_\perp = 0$

Gamma-ray emission from outergap

We assume that electrons radiate γ-rays via curvature radiation in the gap

$$F_{cur}(E_\gamma)^{single} = \frac{\sqrt{3}e^2\gamma_e}{2\pi\hbar s E_\gamma}F(x) \quad (1$$

where γ_e, is determined by $eE_\parallel(z)c = l_{cur} = 2e^2c\gamma_e^4(z)/3s^2$

The total curvature radiation spectrum from the outer gap is given by

$$F_{cur} = \int \frac{dN}{dz}F_{cur}^{single}(z)dz. \quad (1$$

Effects of fitting parameters on spectra ($f=h_2/r_L$, $1-g1, h_1/h_2$)

Roughly speaking the spectrum consist of primary component and screening component, the radiation from primary region is higher energy whereas the screening region with low electric field contributes to low energy part.

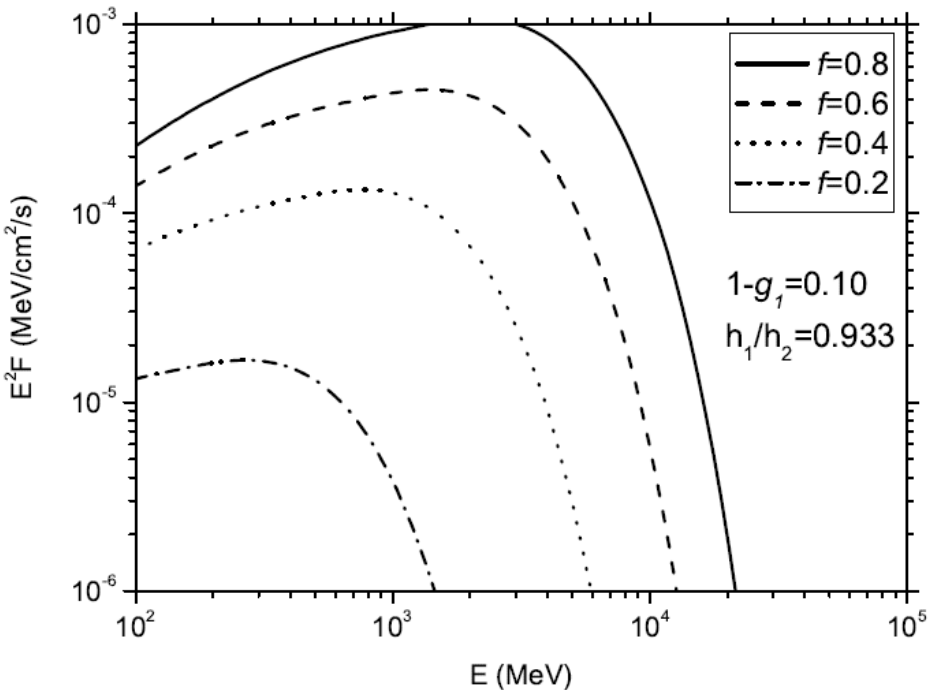

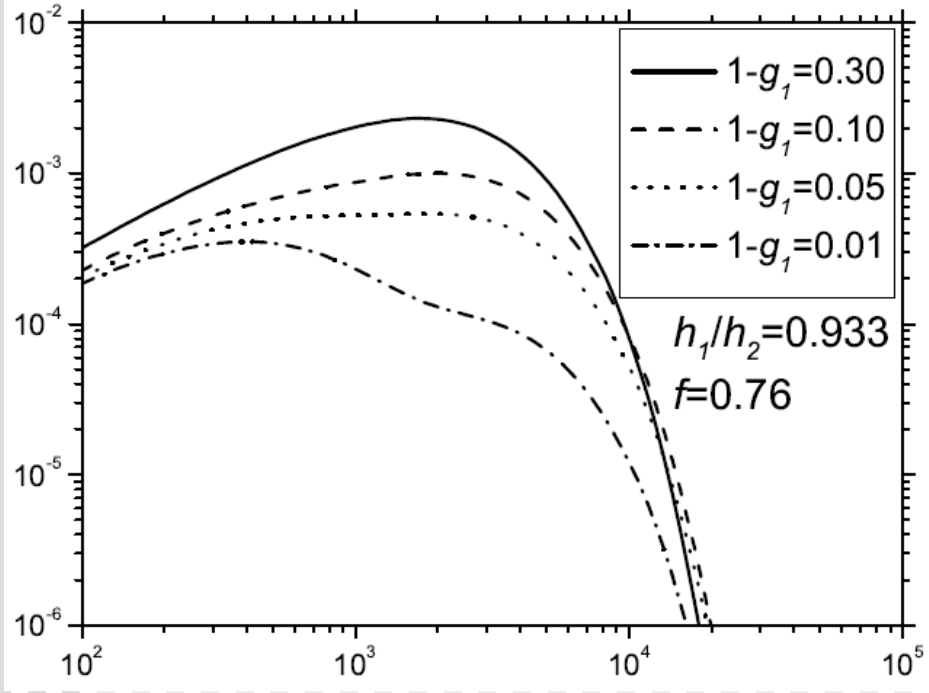

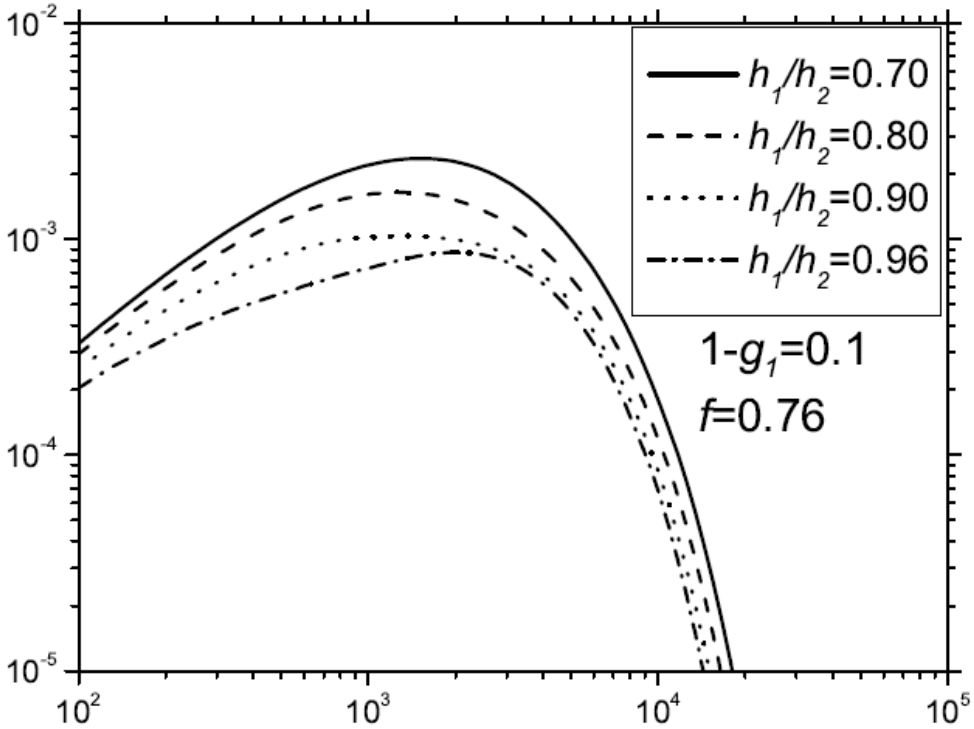

Spectral fits I – EGRET/Fermi pulsars

Solid line is the best model fit. In Vela and Geminga the dashed and dot-dashed line represent the fits by using fitting parameters deviating 10% from the best fit values

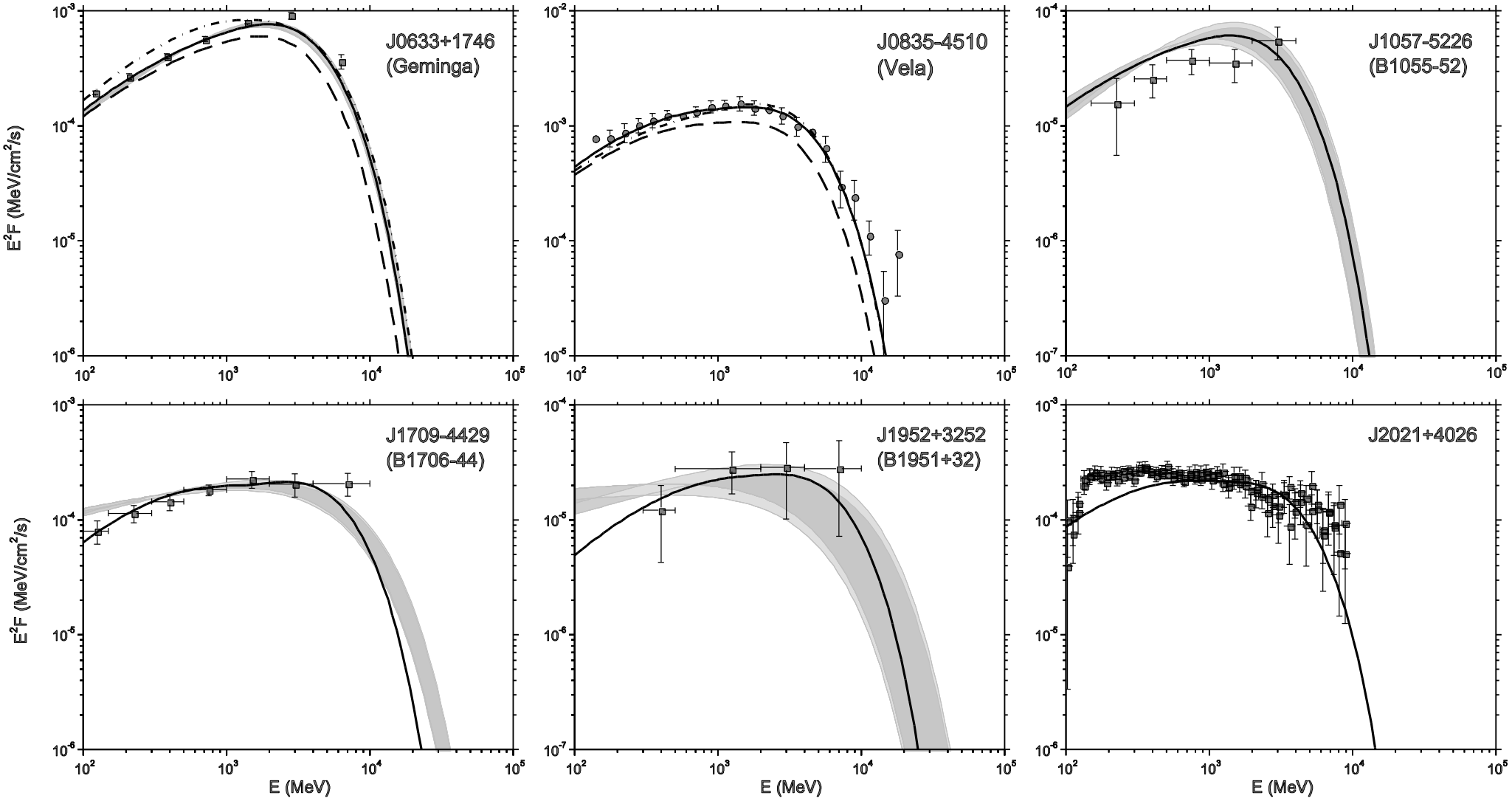

Spectral fits II-MSPs

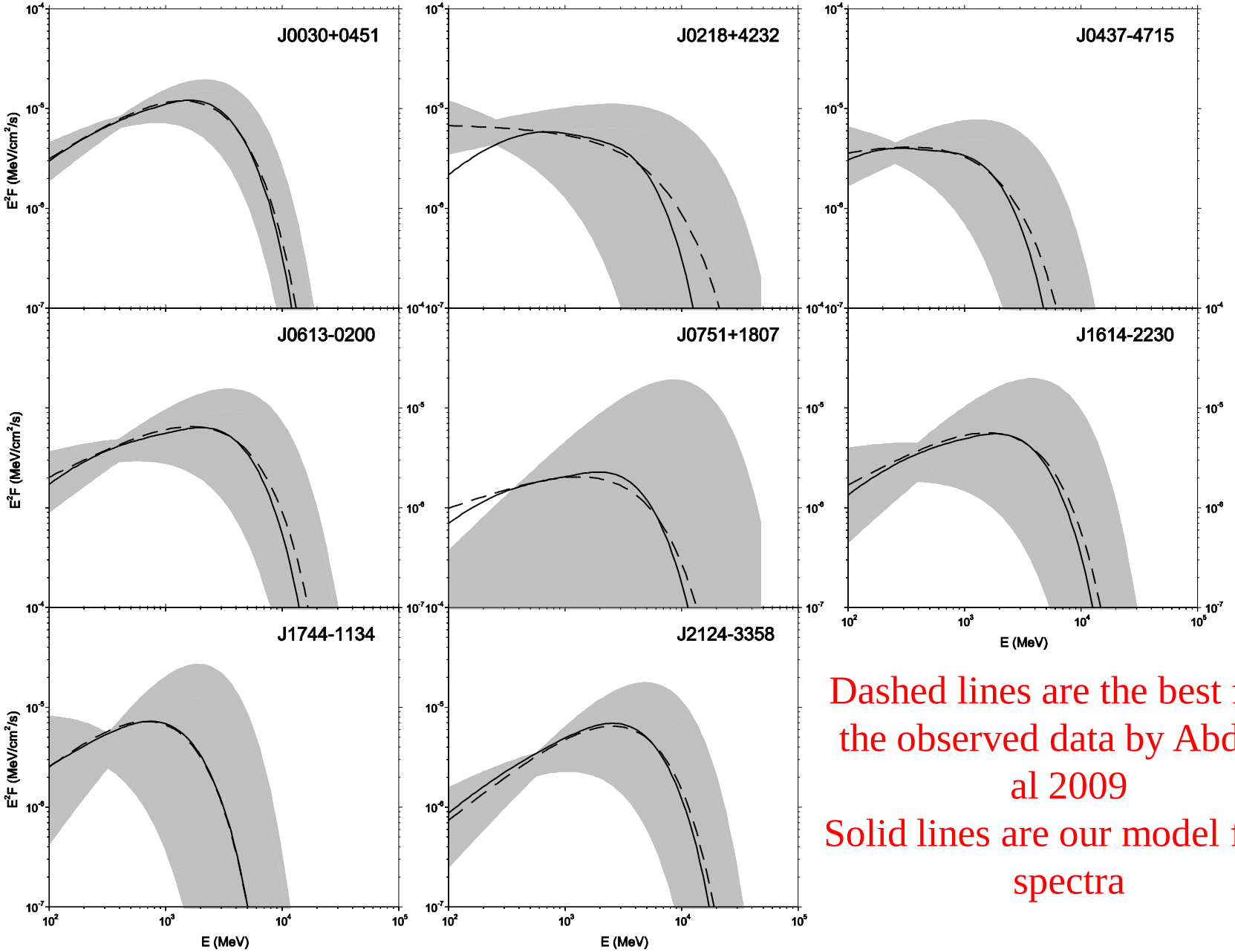

Dashed lines are the best fit of the observed data by Abdo et al 2009

Solid lines are our model fitted spectra

Spectral fits III-other Fermi pulsars

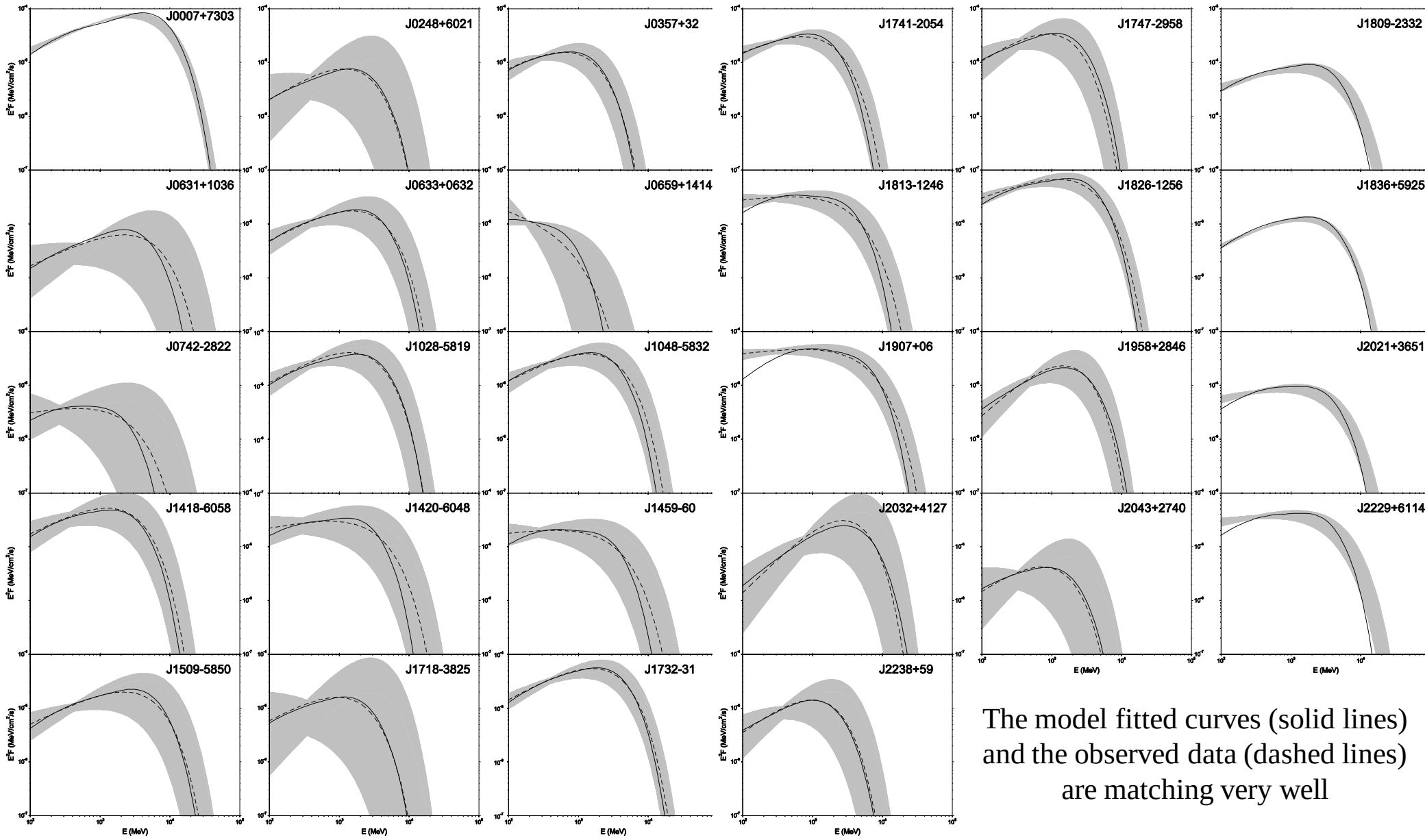

The model fitted curves (solid lines) and the observed data (dashed lines) are matching very well

Distribution of Fitting parameters(f, 1-g1,h1/h2)

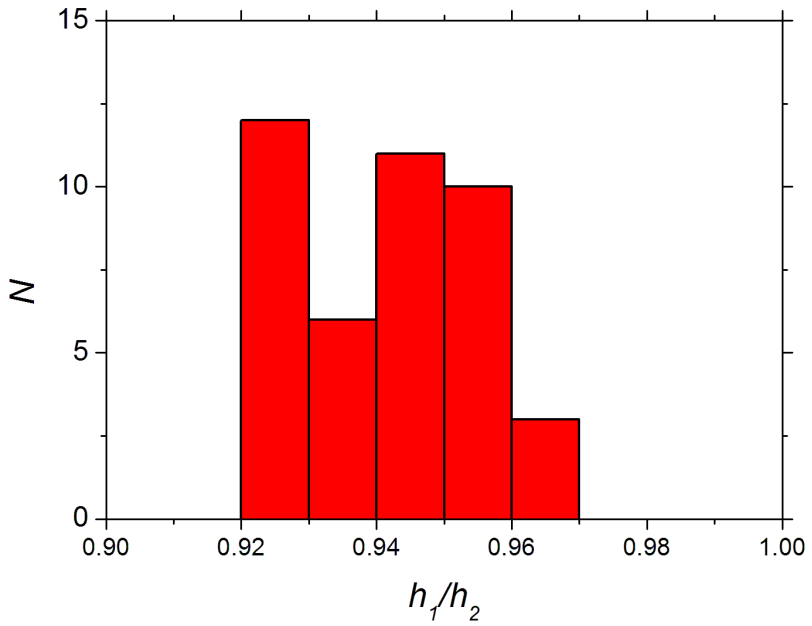

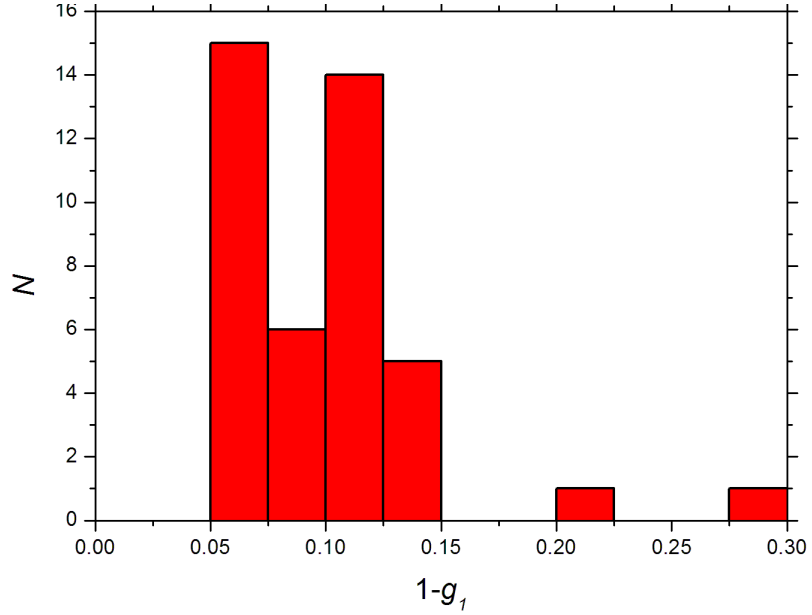

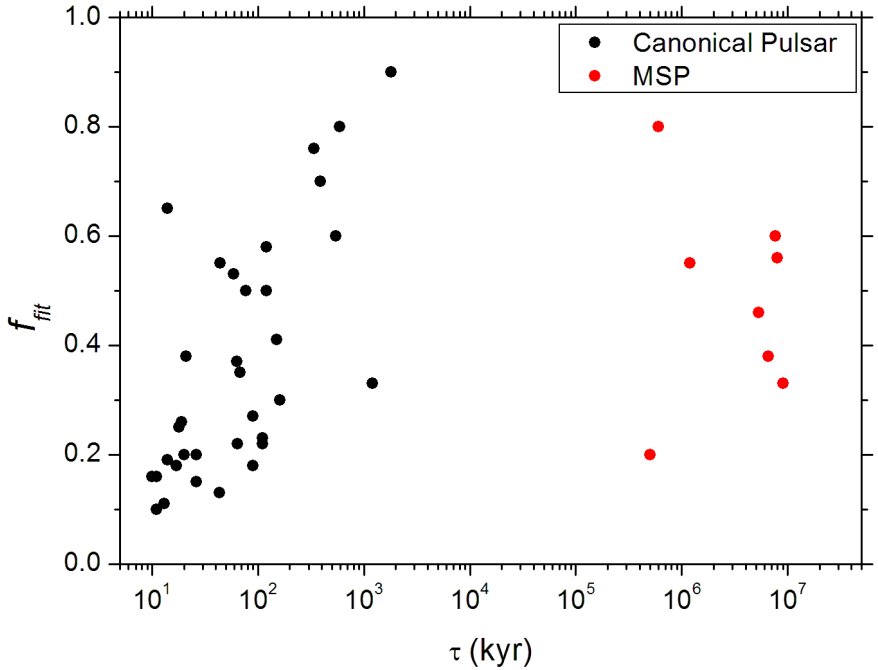

Deduced parameters (η=total gap current, L_γ=predicted γ-ray power)

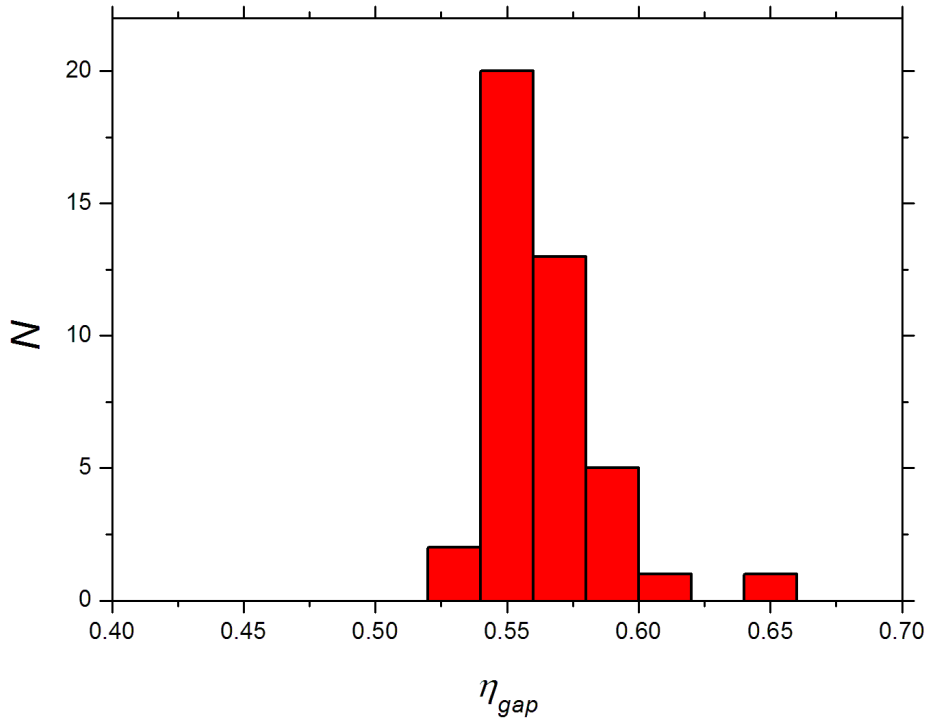

This may suggest a switching of gap closure process at Lsd ~10^{36} erg/s

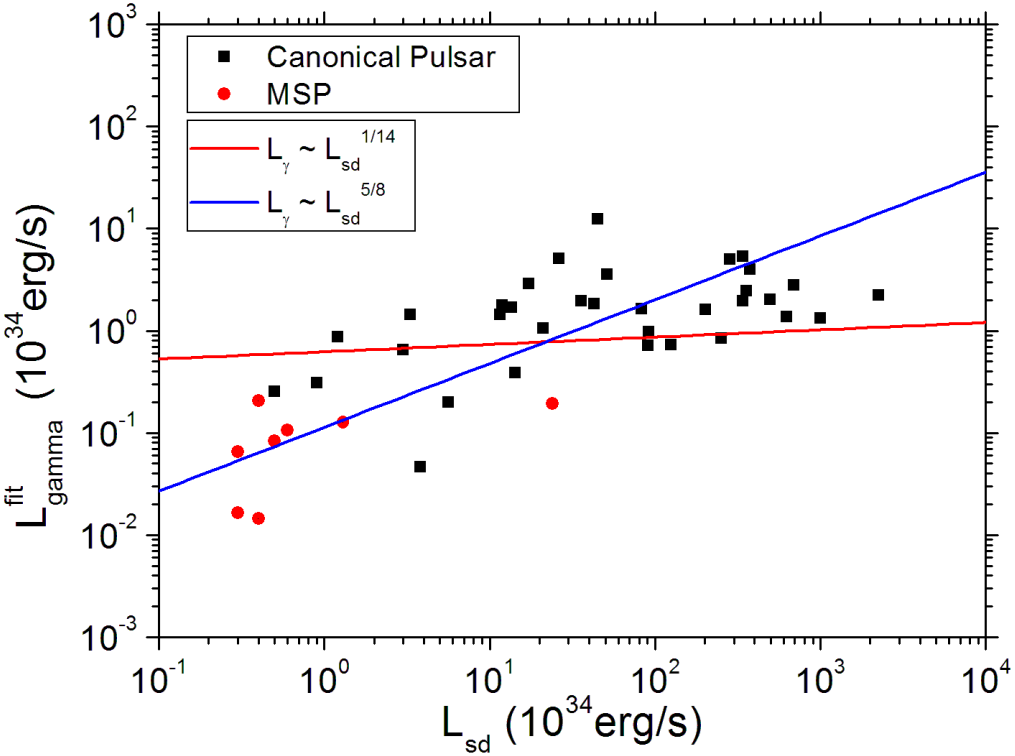

Pair creation processes (Gap Closure Mechanism): photon-photon pair creation

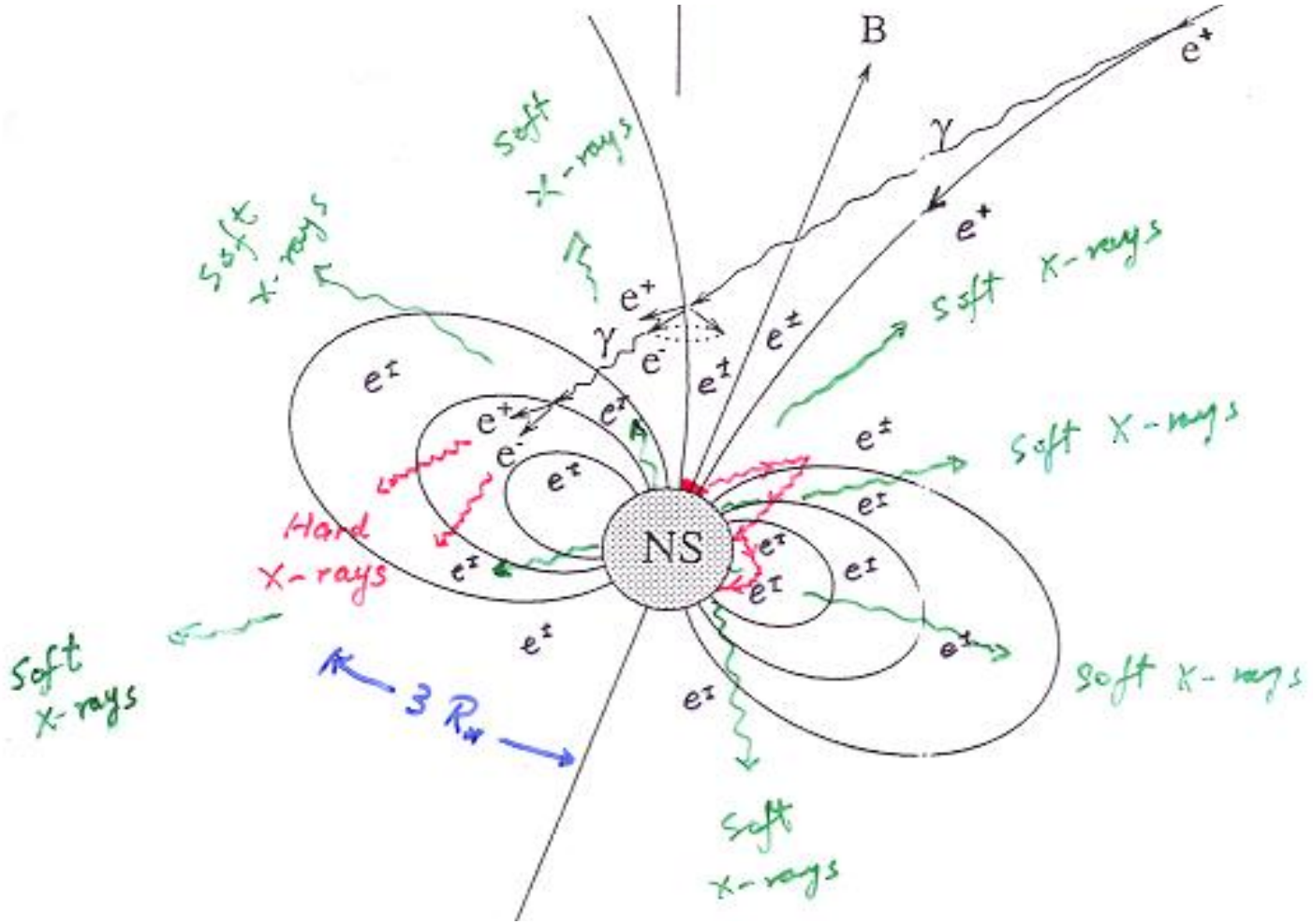

Zhang & Cheng (1997) suggest a self-sustained Mechanism

- In this model, the typical energies of the soft X-rays and the γ-rays are completely determined by pulsar parameters
- Soft X-ray photon:

$$E_X \approx 9.8\times10^{1}\, f^{1/4} B_{12}^{\ 1/4} P^{-5/12} eV$$

- Curvature gamma-ray photon:

$$E_c = E_\gamma \approx 1.4\times10^{8}\, f^{3/2} B_{12}^{\ 3/4} P^{-7/4} eV$$

- Using pair production condition $E_X E_\gamma \sim (m_e c^2)^2$ outergap size :

$$f \approx 5.5 B_{12}^{\ -4/7} P^{26/21}$$

This model predicts $L_\gamma \approx f^3 L_{sd} \sim (L_{sd})^{1/14} B^{1/7}$ and

$$E_c \sim (L_{sd})^{3/112} B^{-3/56}$$

Insensitive to pulsar parameters

magnetic pair creation

Recently, we (Takata etal. 2010) argue that because the electric field from the null surface to the star is too weak to compensate the energy loss of the charged particles, then the characteristic curvature photon energy emitted near the star, where the field may be dominated by surface field, is independent of pulsar parameters and given by

$$m_e c^2/\alpha_f \sim 100\mathrm{MeV}.$$

These photons cannot be converted into pairs by thermal X-rays but they are energetically enough to become pairs via the magnetic pair creation process at a distance R_i ~(2-3)R_s. Using the condition of magnetic pair creation we show that the magnetic pair creation process can take place at the height from the closed field lines

$$h_{\perp,m}(R_i) \sim 10^4 \chi_{-1}^2 B_{m.12}^{-2} s_7 \ \mathrm{cm},$$

where $\chi_{-1} = \chi/0.1$, $B_{m,12}$ is the strength of the magnetic field at pair creation region. We can rescale to get $h_\perp(R_s, m) \sim (R_s/R_i)^{3/2} h_{\perp,m}(R_i)$

However this pair creation process cannot constraint the gap size because the created pairs are moving toward the star and cannot provide screening of the gap.

Magnetic pair creation and strong surface magnetic field

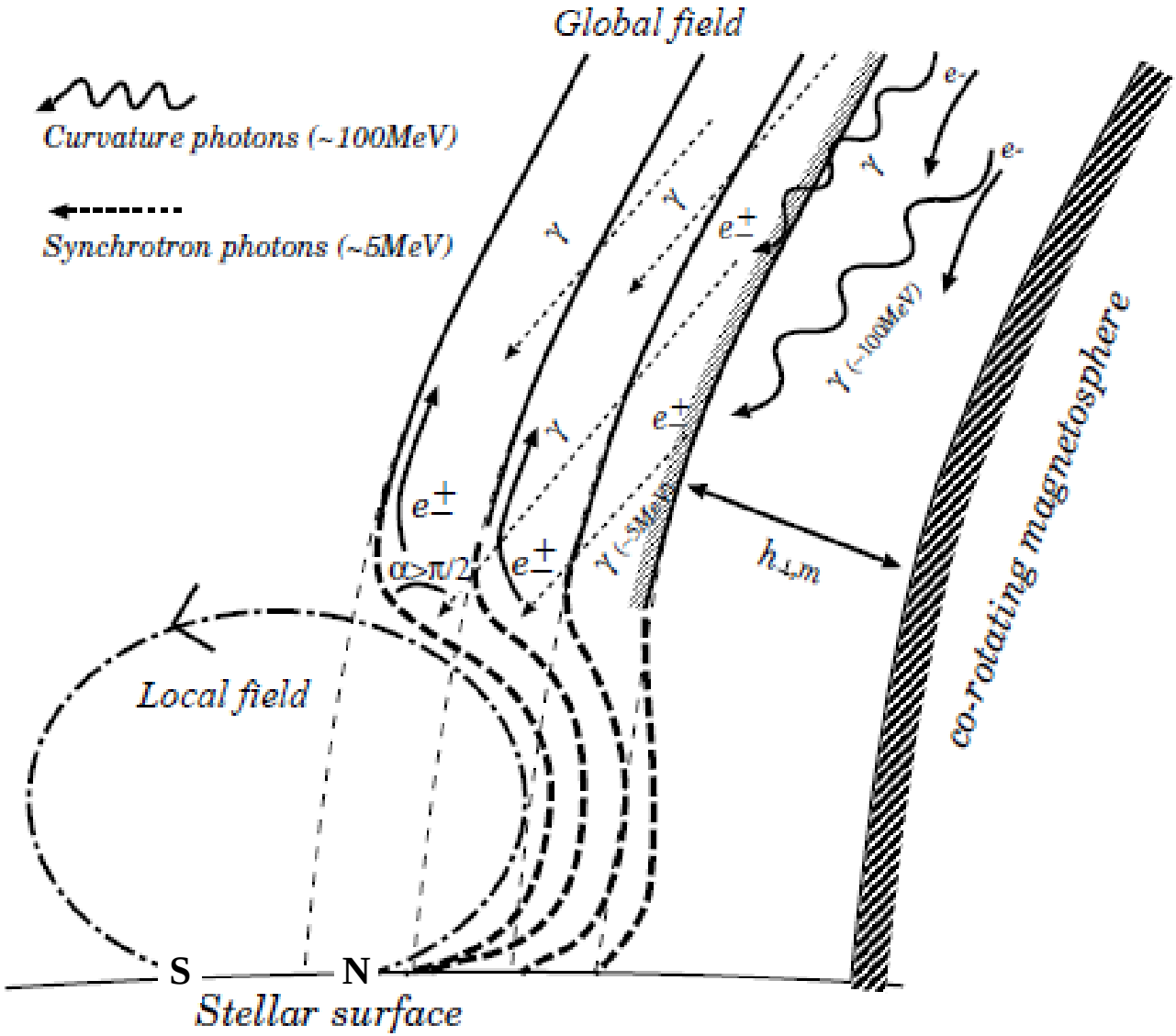

The photon multiplicity is of order of 10^5, only a very tiny fraction of these photons converted into pairs in these sideward bending field lines is sufficient to screen out the electric field of the gap in the outermagnetospheric region and this can provide an alternative condition to determine the outergap size, i.e. the outergap size determined by magnetic pair creation is

$$f_m \equiv \frac{h_{\perp,m}(R_s)}{r_p} \sim 0.25 K(\chi, B_m, s) P_{-1}^{1/2},$$

$$K = \chi_{-1}^2 B_{m,12}^{-2} s_7 \left(\frac{R_s}{R_i}\right)^{3/2}$$

Furthermore if the surface field is sufficiently strong then the quantities, i.e. B_m, s *and* $R_i(B_m,m)$ are determined by the surface field instead of the dipolar field. In other words they are local quantities and independent of pulsar parameters. We assume $K \sim const.$

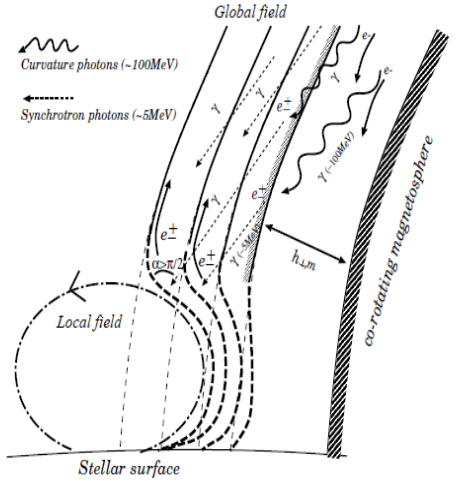

Model predictions I

Once the outergap size is known, we can estimate the gamma-ray power

$$L_\gamma(K, B_d, P) \sim I_{gap} V_{gap} \sim (f_m I_{GJ})(f_m^2 V_{tot}) \sim 2 \times 10^{33} K^3 B_{d,12}^2 P_{-1}^{-5/2} \text{ erg/s}.$$

And the characteristic energy in the outergap is

$$E_c(K, B_d, P) = \frac{3}{4\pi} \frac{hc\gamma^3}{s} \sim 0.55 K^{3/2} B_{d,12}^{3/4} P_{-1}^{-1} \text{ GeV}.$$

Here *K is an unknown const. depending on surface magnetic field properties. However K should not be the same for canonical pulsars and millisecond pulsars, we can estimate K~1 (B_m ~10^{13}G >$B_{d,12}$ ~3 and m=2)for canonical pulsars and K~10 (B_m ~10^{11}G, which is the minimum field to convert 100MeV photons) for MSPs.*

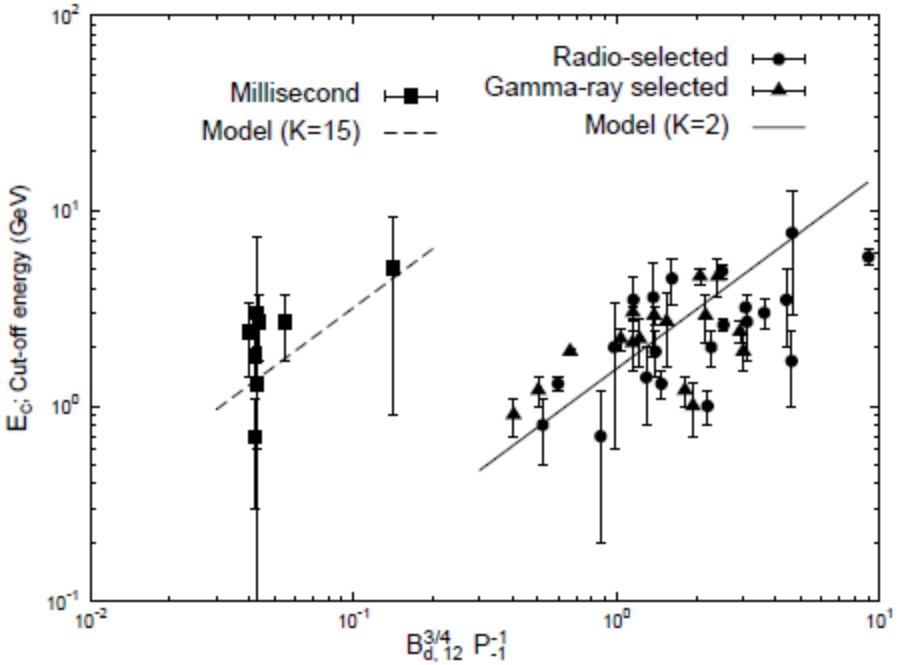

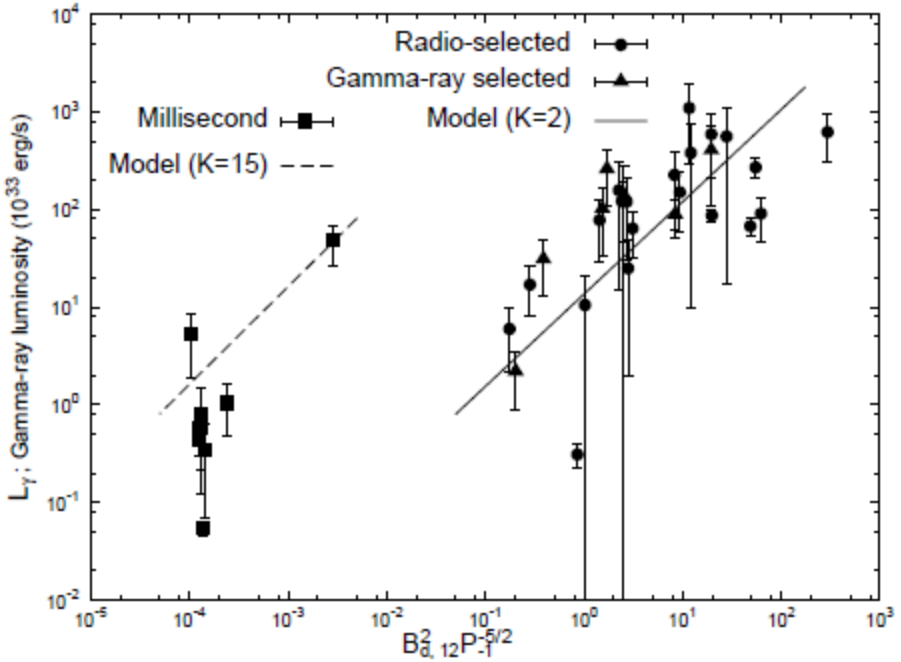

Model predictions II

It is interesting to note that we can eliminate K from L_γ and E_c as

$$\frac{L_\gamma}{E_c^2} \sim 6.6 \times 10^{34} B_{d,12}^{1/2} P_{-1}^{-1} \text{ erg/s GeV}^2$$

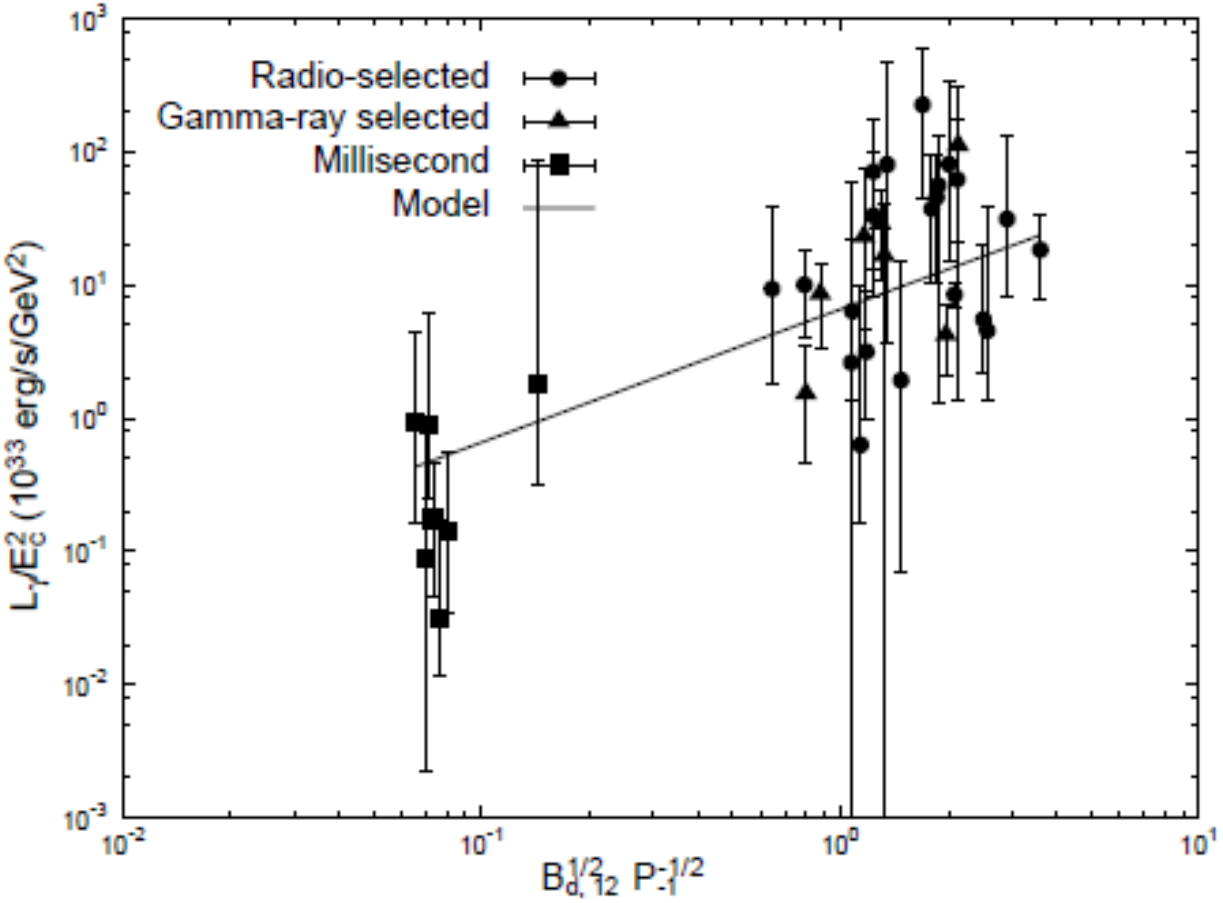

Model predictions III

We can also express L_γ and E_c in terms of spin-down age τ as

$$L_\gamma \sim 10^{36} K^3 B_{d,12}^{-1/2} \tau_3^{-5/4} \text{ erg/s} \qquad E_c \sim 7 K^{3/2} B_{d,12}^{-1/4} \tau_3^{-1/2} \text{ GeV}$$

for $K = 2$ and the typical magnetic field of $< B_{d,12} >= 3$ for the canonical pulsars

for $K = 15$ and $< B_{d,12} >= 3 \times 10^{-4}$ for the millisecond pulsars

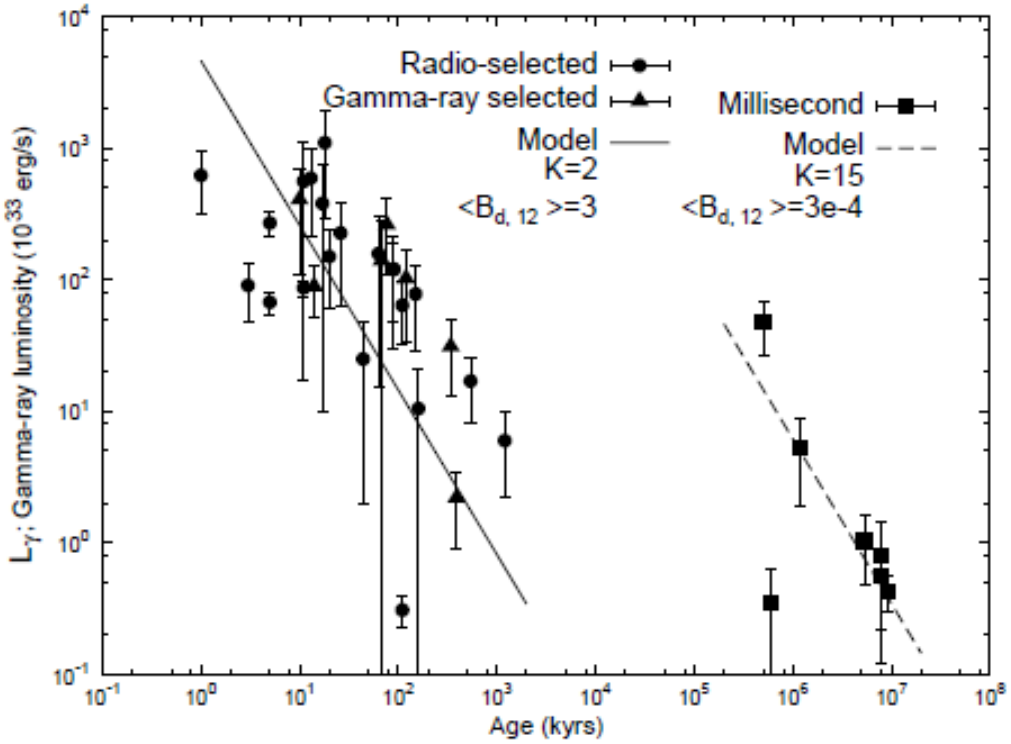

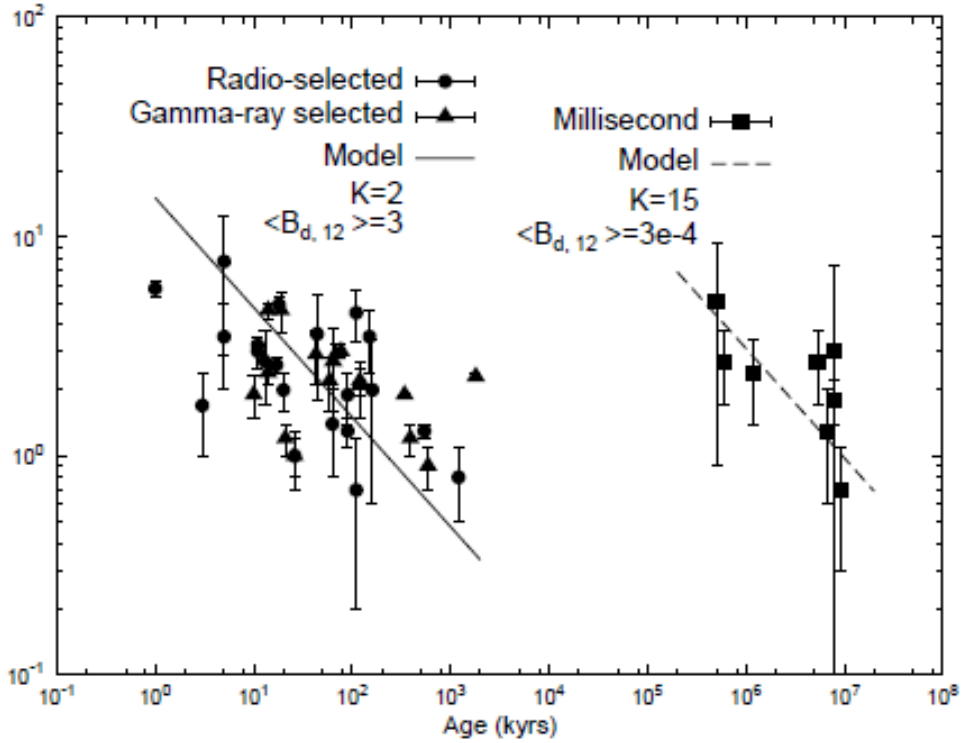

Model predictions IV

We can also express L_γ and E_c in terms of spin-down power L_{sd} as

$$L_\gamma \sim 2 \times 10^{32} K^3 B_{d,12}^{3/4} L_{sd,34}^{5/8}, \ \mathrm{erg/s} \qquad E_c \sim 0.22 K^{3/2} B_{d,12}^{1/4} L_{sd,34}^{1/4} \ \mathrm{GeV}$$

for $K = 2$ and the typical magnetic field of $< B_{d,12} >= 3$ for the canonical pulsars
for $K = 15$ and $< B_{d,12} >= 3 \times 10^{-4}$ for the millisecond pulsars

It turns out that the numerical values of $K^{3/2} B_{d,12}^{1/4}$ and $K^3 B_{d,12}^{3/4}$ for canonical pulsars and MSPs are only differs by a factor of 2.

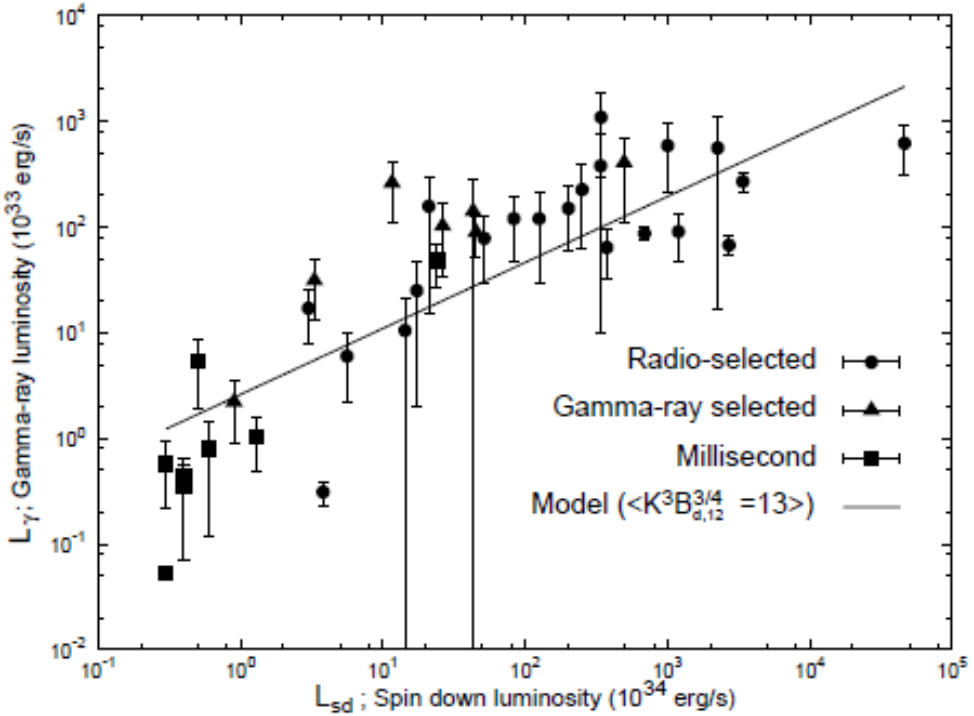

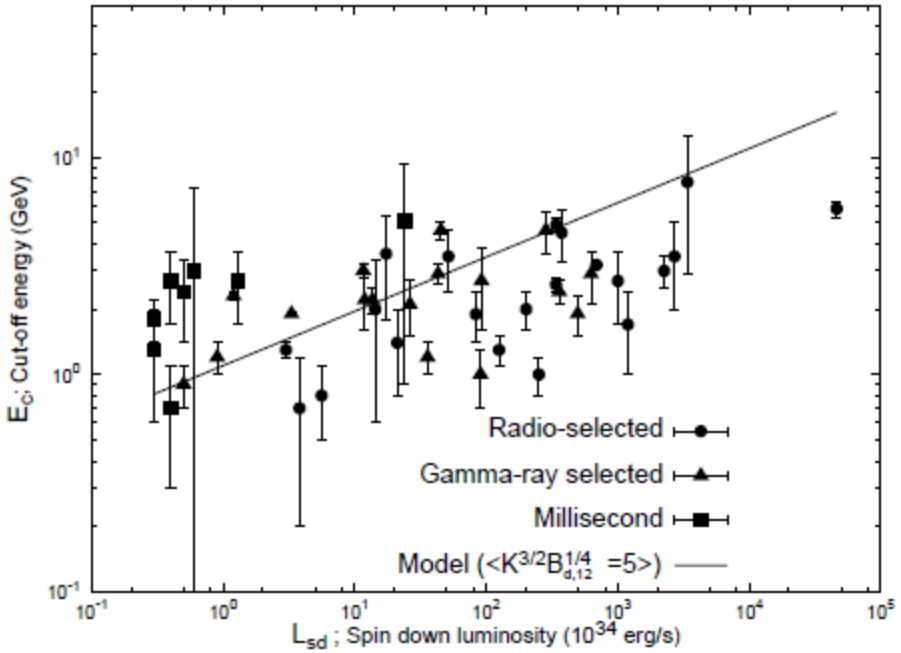

Summary

- A 2D outergap model with a primary region plus a screening region can explain the phase average spectrum of all mature pulsars detected by Fermi very well.
- The fitting results indicate that the primary region consists of 10% GJ current and the screening region contains 40%. The low current in primary region ensures the production of multi-GeV photons and hence pair creation can take place. Furthermore the screening region can have charge density even higher than the Goldreich-Julian value, which can explain why some pulsars can have a very flat spectrum.
- L^{fit}_{γ} vs L_{sd} suggests two possible pair creation processes, i.e. photon-photon pair creation and magnetic pair creation. The transition takes place when the efficiency of these processes equal,i.e.

$$f_{ZC} = f_m, \text{ which gives } L_{sd} \sim 10^{36} K^{-84/31} B_{12}^{-34/31} \text{erg/s}$$

- The magnetic pair creation closure process also predicts that

$$L_\gamma \propto L_{sd}^{5/8} \text{ or } L_\gamma \propto \tau^{-5/4}, \text{ and } E_c \propto L_{sd}^{1/4} \text{ or } E_c \propto \tau^{-1/2}$$

Gamma-rays from Globular clusters (GCs)

- It is generally assumed that gamma-rays from GCs come from the magnetosphere of MSPs in GCs within the light cylinder
- However we have some reasons to speculate that at least most MSPs in GCs do not have strong particle accelerators.

(1)28 MSPs are detected by Fermi but none of them is in GCs

(2)The X-ray spectrum of MSPs in GCs can be described by a thermal spectrum with characteristic temperature almost constant and their L_x and L_sd relation differs from that of MSPs in the field (Cheng & Taam 2003)

(3)No signature of non-thermal X-rays resulting from PWN in GCs (Hui, Cheng and Taam 2009)

(4)Hui, Cheng & Taam (2010) find that the radio cumulative distribution functions for MSPs in GCs differ from that of MSPs in the field

(5)Kong, Hui & Cheng (2010) find that there are significant contribution of photon with energies >10GeV in Terzan 5

(6)In Mal. Ruderman's talk next week he can tell you why the field structure in these two population of MSPs should be different

Inverse Compton Model

- We have proposed an alternative model to explain the gamma-ray emission from GCs, i.e. gamma-rays are produced by inverse Compton scattering between the relativistic electrons/positrons in pulsar wind and the background soft photons including, the optical photons in GC, Optical photons and IR photons from the galactic plane, and CMB photons. We can fit the observed gamma-ray spectrum very well.
- Most important if this model is true then it predicts that

  L_gamma ~ (N_msp)(energy density of soft photons)

R=0.69

R=0.79

R=-0.28

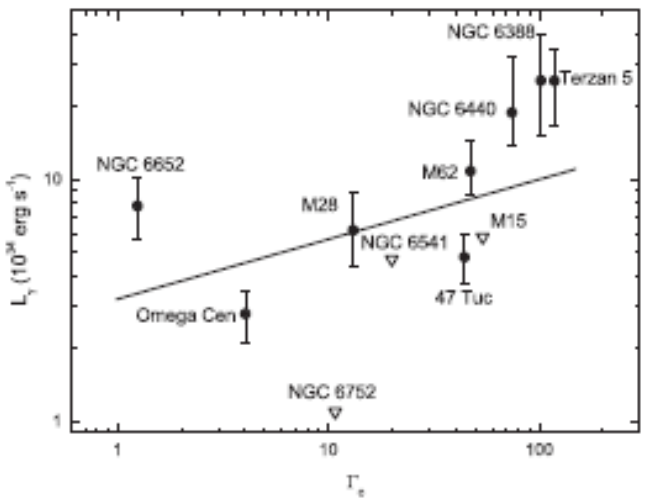

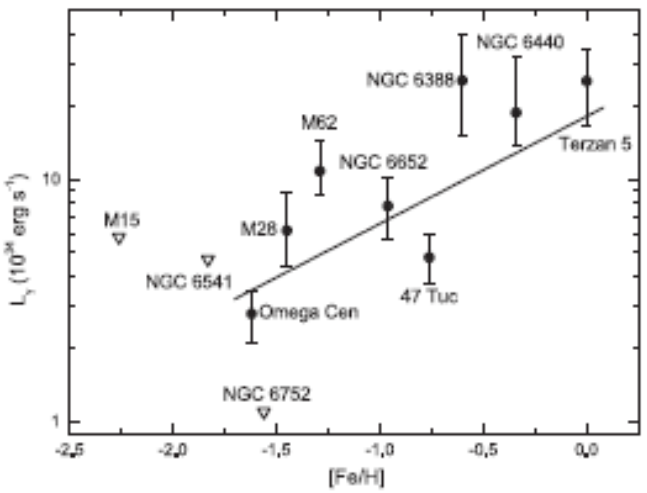

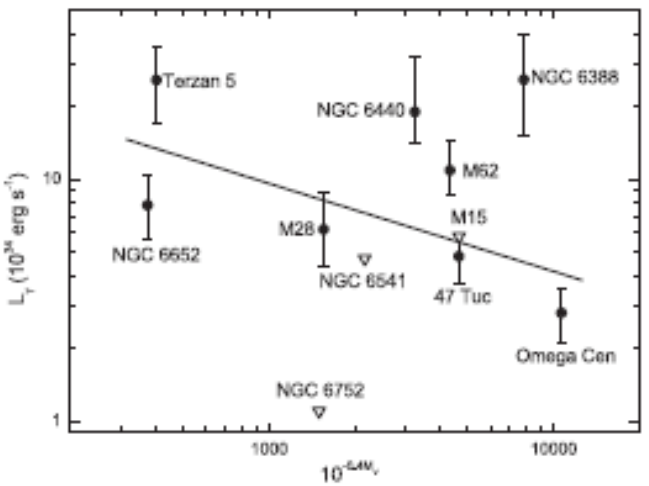

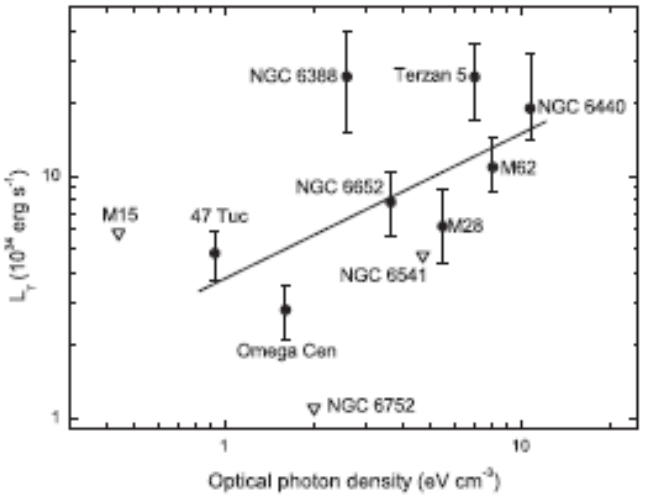

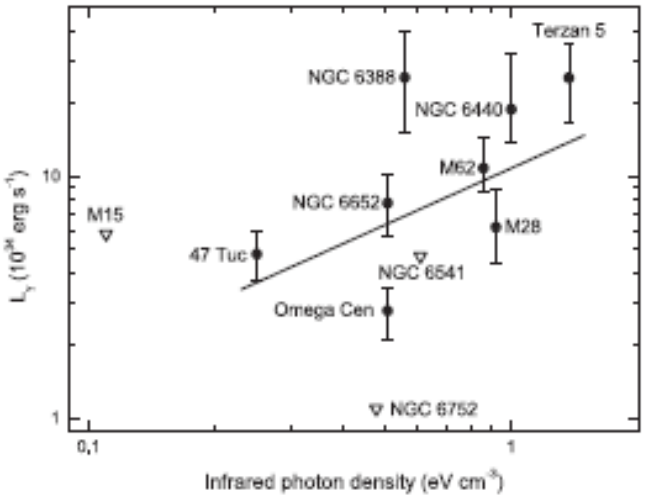

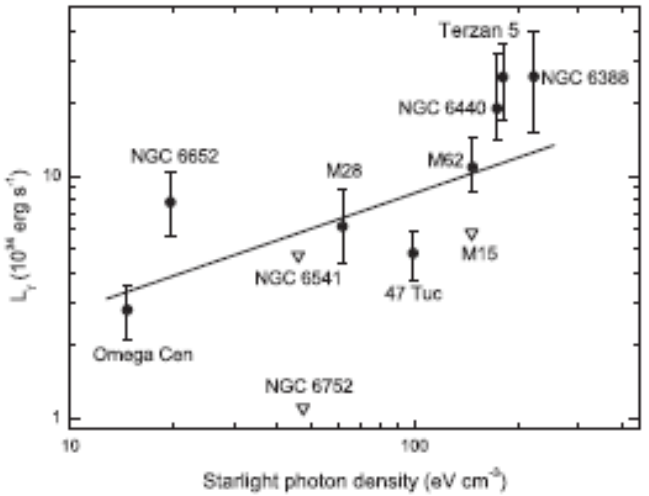

R=0.60

R=0.58

R=0.79

Remark: the star light photon density and number of MSPs are not independent quantity

R=0.80

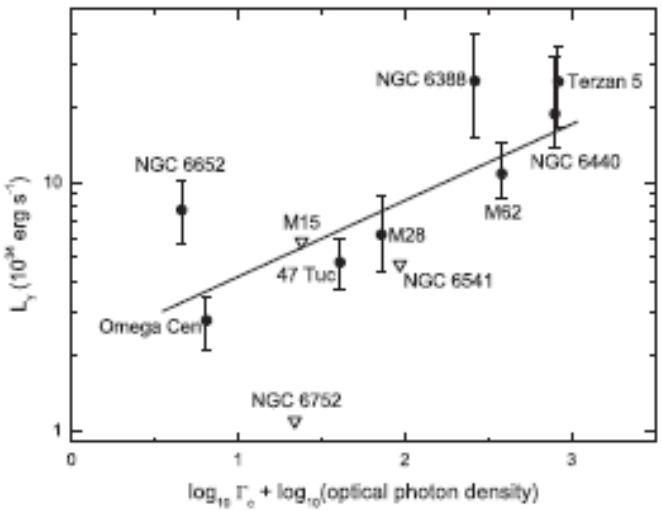

R=0.77

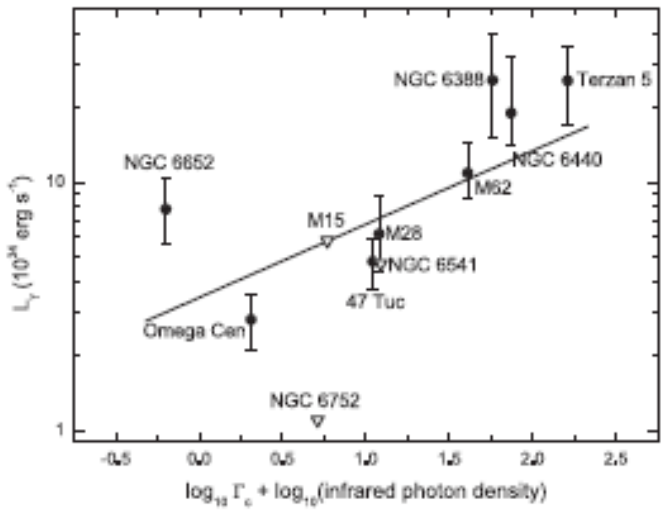

R=0.74

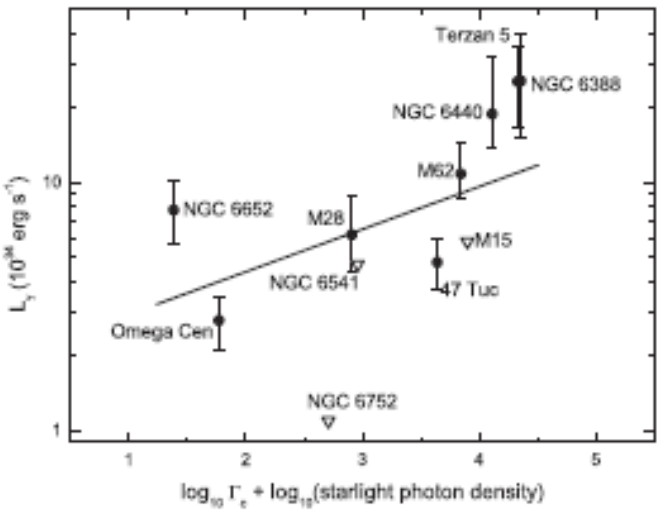

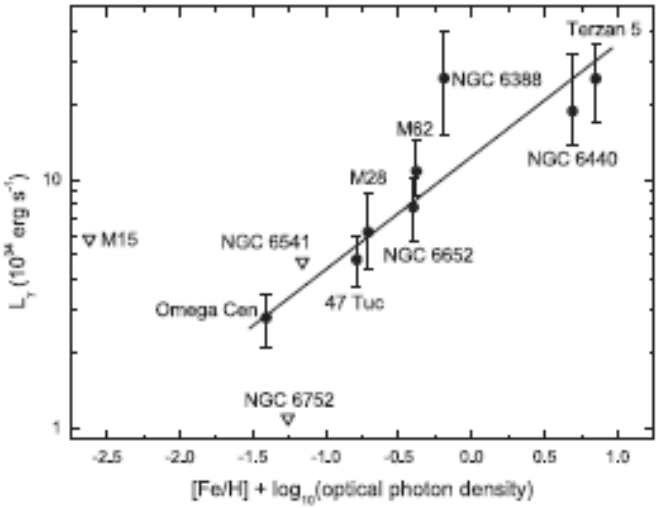

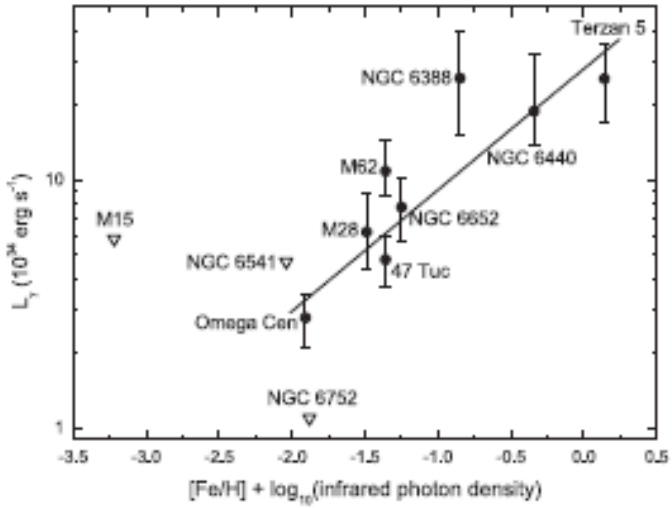

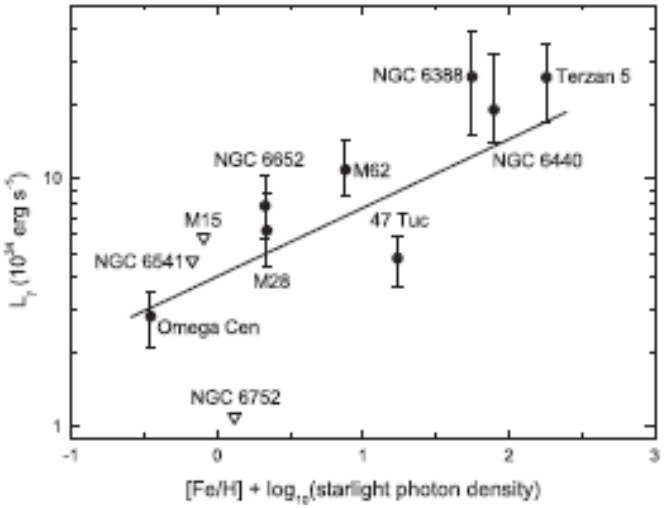

R=0.89

R=0.87

R=0.87

Remark: the star light photon density and number of MSPs are not independent quantity